ACS Chemical Neuroscience

Research Article

pubs.acs.org/chemneuro

Benzodiazepinone Derivatives Protect against Endoplasmic Reticulum Stress-Mediated Cell Death in Human Neuronal Cell Lines

Haixia Zou,[†] Allison S. Limpert,[†] Jiwen Zou,[‡] Anna Dembo,[†] Pooi-San Lee,[†] Daniel Grant,[†] Robert Ardecky,[‡] Anthony B. Pinkerton,[‡] Gavin K. Magnuson,[‡] Mark E. Goldman,[†] Juan Rong,[†] Peter Teriete,[†] Douglas J. Sheffler,[†] John C. Reed,[†] and Nicholas D. P. Cosford*[,†,‡]

[†]Cell Death and Survival Networks Research Program, NCI-Designated Cancer Center, and [‡]Conrad Prebys Center for Chemical Genomics, Sanford-Burnham Medical Research Institute, 10901 North Torrey Pines Road, La Jolla, California 92037, United States

Supporting Information

ABSTRACT: Endoplasmic reticulum (ER) stress causes neuronal dysfunction followed by cell death and is recognized as a feature of many neurodegenerative diseases. Using a phenotypic screen, we recently identified benzodiazepinone derivatives that reduce ER stress-mediated apoptosis in a rat neuronal progenitor cell line (CSM14.1). Herein we describe how structure−activity relationship (SAR) studies around these screening hits led to compounds that display robust cytoprotective activity against thapsigargin-induced ER stress in SH-SY5Y and H4 human neuronal cell lines. We demonstrate that the most potent of these derivatives, compound **4hh**, inhibits the activation of p38 MAP kinase (p38) and c-Jun N-terminal kinase (JNK), protein kinases that are downstream signal effectors of the unfolded protein response (UPR). Compound **4hh** specifically protects against thapsigargin-induced cell death and displays no protection against other insults known to induce cellular stress or activate p38. However, compound **4hh** provides moderate inhibition of p38 activity stimulated by compounds that disrupt calcium homeostasis. Our data indicate that probe compound **4hh** is a valuable small molecule tool that can be used to investigate the effects of ER stress on human neurons. This approach may provide the basis for the future development of therapeutics for the treatment of neurodegenerative diseases.

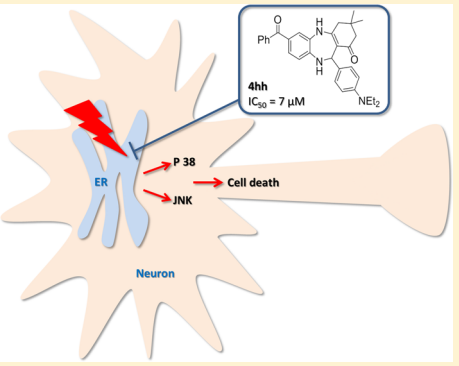

KEYWORDS: *Benzodiazepinone, ER stress, p38 MAPK, calcium homeostasis, neurodegeneration, thapsigargin*

Cell death induced by endoplasmic reticulum (ER) stress is a critical component of many disorders including diabetes, cardiovascular disease, ischemic insult, and prion disease.[1−3] Additionally, many devastating neuronal disorders are characterized by proteinopathies that upregulate the unfolded protein response (UPR). The UPR cell signaling mechanism activates ER stress pathways that eventually lead to neuronal death. Thus, ER stress is implicated in several neurodegenerative disorders that have limited treatment options, including Alzheimer's disease, Parkinson's disease, Huntington's disease, and amyotrophic lateral sclerosis (ALS).[3,4] Consequently, the identification of novel compounds that ameliorate ER stress and reduce cellular apoptosis may have clinical relevance for the treatment of numerous disease states.

The ER is the organelle responsible for accurate protein folding, which is achieved through post-translational modifications of the amino acid chain. The ER can undergo stress if subjected to a variety of physiological insults, including accumulation of misfolded proteins, misglycosylation of proteins, dysregulation of calcium, and oxidative stress.[5] These pathological conditions stimulate the UPR, an adaptive process that leads to the reduction of protein synthesis and the upregulation of molecular chaperones. In the event of the failure of these processes to alleviate ER stress, apoptotic pathways are initiated.

ER stress stimulates the activation of three distinct signaling pathways to elicit cellular adaptation or cell death (Figure 1).[2] These separate pathways are initiated by three transmembrane proteins: protein kinase R (PKR)-like ER kinase (PERK), activating transcription factor 6 (ATF6), and inositol-requiring enzyme 1 (IRE1).[6] When cell stress remains unresolved, IRE1 complexes with the adaptor molecule tumor necrosis factor receptor-associated factor 2 (TRAF2), which then binds apoptosis signal regulating kinase 1 (ASK1), a mitogen-activated protein (MAP) kinase kinase kinase. This IRE1-TRAF2-ASK1 complex promotes activation of the proapoptotic signaling proteins p38 MAP kinase (p38) and c-Jun N-terminal kinase (JNK).[7,8] p38 is able to induce cell death through the phosphorylation of two serine residues (78 and 81) on the transactivation domain of the transcription factor C/EBP homologous protein (CHOP). This phosphorylation event increases CHOP transcriptional activity, which upregulates the

Received: November 21, 2014
Revised: December 23, 2014
Published: December 29, 2014

DOI: 10.1021/cn500297v
ACS Chem. Neurosci. 2015, 6, 464−475

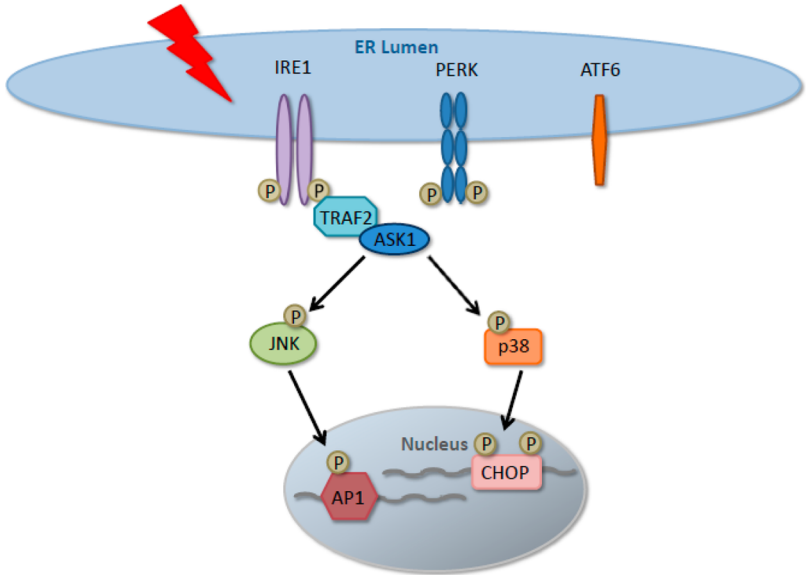

Figure 1. ER stress activates p38 and JNK through an IRE1/TRAF2/ASK1-mediated signaling pathway. ER stress elicits the activation of three resident ER transmembrane proteins including IRE1. IRE1 complexes with TRAF2 and ASK1, allowing for the stimulation of JNK and p38. JNK and p38 phosphorylate and activate the transcription factors AP1 and CHOP, respectively.

expression of apoptotic genes.[3,9] Activation of JNK results in the phosphorylation of transcription activator protein 1 (AP1) which also induces the expression of inflammatory and proapototic genes (Figure 1).[10]

The natural product thapsigargin (Figure 2) is one of a number of chemical agents that induce ER stress and activate

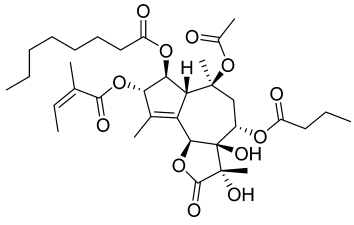

Figure 2. Structure of thapsigargin.

the UPR in cells.[11] Thapsigargin initiates ER stress through inhibition of sarco/endoplasmic reticulum Ca^{2+} ATPase (SERCA) calcium transporters that facilitate calcium entry into the ER. This causes a depletion of ER calcium stores and an elevation of cytosolic calcium levels. As many ER chaperones depend on ER Ca^{2+} ions for proper functioning, disruption of ER Ca^{2+} concentrations results in ER stress.[12] Disruptions in calcium regulation are also observed in many neuronal disorders. Calcium is an essential second messenger involved in cellular signaling, and tight control over the concentration of Ca^{2+} ions is especially important in neuronal cells to maintain membrane excitability and to allow depolarization. Importantly, the dysregulation of calcium homeostasis has been identified as a component of neurodegenerative diseases such as Alzheimer's disease.[13−15]

The upregulation of ER stress pathways is a common characteristic of many neurodegenerative diseases. ER stress and activation of the UPR have been observed in Alzheimer's disease patients[16] where the accumulation of amyloid beta protein contributes to cellular dysfunction.[12] In addition, the E3 ubiquitin ligase Parkin has been demonstrated to alleviate ER stress in neurons, and mutations in this protein have been characterized as the predominant cause of Parkinson's disease.[17] Furthermore, familial ALS is frequently caused by mutations in superoxide dismutase 1 (SOD1) that cause this protein to form toxic aggregates in the ER.[18,19] Treatments for Alzheimer's disease, Parkinson's disease, and ALS are extremely limited, and therefore, the discovery and characterization of compounds that modulate ER stress mechanisms would represent an important step toward the development of therapeutics for these disorders.

We recently reported a high-throughput screen (HTS) performed through the Molecular Libraries Probe Production Center Network (MLPCN) using a phenotypic cell-based assay to identify small molecule compounds that rescue a rat neuronal cell line (CSM14.1) from cell death induced by thapsigargin.[20] In these studies, we demonstrated that certain benzodiazepinone screening hits (Figure 3) reduce ER stress-

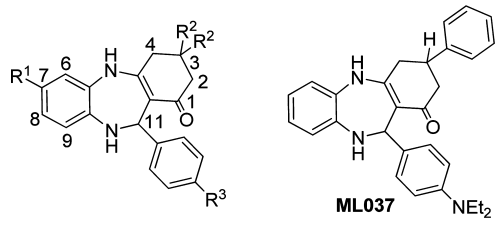

Figure 3. Structure of benzodiazepinone hits from phenotypic screening and initial MLPCN probe compound ML037.

induced cell death in rodent neuronal cell lines and cultured neurons. These active benzodiazepinone derivatives specifically inhibited stress signals propagated through ASK1 kinase by enhancing the association of ASK1 with 14−3−3 proteins, thereby reducing its ability to bind to and activate downstream effectors of cell stress, such as p38 and JNK.[20] However, these compounds appear to have no direct effect on ASK1 kinase activity or the activity of over 400 kinases tested.[20] In addition, the benzodiazepinone hits were shown to exhibit cytoprotective activity against ER stress mediated by thapsigargin, but not staurosporine, VP16, or TNF, in human cervical (HeLa),

DOI: 10.1021/cn500297v
ACS Chem. Neurosci. 2015, 6, 464−475

Table 1. Cytoprotective Activity of Benzodiazepinone Analogues toward Human Neuronal Cells[a]

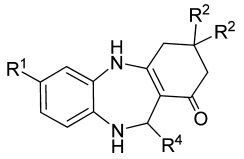

CPD #	R^1	R^4	R^2	SH-SY5Y MAX ± SEM (% Viability)	H4 MAX ± SEM (% Viability)
1% DMSO				100.0 ± 1.8	100.0 ± 5.6
7.5 μM Tg				5.5 ± 0.4	1.1 ± 0.1
Salubrinal				34.0 ± 0.9	14.0 ± 1.2
4a	Cl		H	3.7 ± 0.5	0.5 ± 0.1
4b	Cl		H	2.8 ± 0.1	0.6 ± 0.1
4c	Cl		H	2.4 ± 0.0	0.3 ± 0.1
4d	Cl		H	2.5 ± 0.2	0.6 ± 0.4
4e	Cl		H	4.4 ± 0.3	2.4 ± 0.1
4f	Br		H	2.1 ± 0.0	0.3 ± 0.4
4g	Br		H	2.2 ± 0.4	0.1 ± 1.0
4h	Br		H	1.9 ± 0.1	1.2 ± 0.2
4i	Br		H	3.8 ± 0.3	1.7 ± 0.1
4j	CF_3		H	18.6 ± 0.9	1.8 ± 0.9
4k	CF_3		H	19.8 ± 1.0	11.5 ± 3.3
4l	CF_3		H	7.1 ± 0.1	2.2 ± 0.1
4m	Cl		CH_3	0.0 ± 1.1	0.7 ± 0.4
4n	Cl		CH_3	6.8 ± 0.7	8.1 ± 1.4
4o	Cl		CH_3	17.4 ± 0.0	7.8 ± 0.1
4p	Cl		CH_3	3.8 ± 0.0	6.1 ± 0.8
4q	Cl		CH_3	4.4 ± 0.4	0.7 ± 0.3
4r	Cl		CH_3	7.5 ± 0.2	7.4 ± 0.1

CPD #	R^1	R^4	R^2	SH-SY5Y MAX ± SEM (% Viability)	H4 MAX ± SEM (% Viability)
4s	Br		CH_3	14.2 ± 0.1	64.8 ± 1.2
4t	Br		CH_3	38.9 ± 0.6	14.3 ± 0.4
4u	Br		CH_3	17.3 ± 2.8	12.0 ± 0.1
4v	Br		CH_3	6.2 ± 0.7	0.6 ± 0.3
4w	Br		CH_3	16.7 ± 0.5	12.8 ± 1.3
4x	Ph		CH_3	45.5 ± 0.1	28.8 ± 3.8
4y	Ph		CH_3	49.3 ± 1.6	31.6 ± 0.9
4z	Ph		CH_3	49.6 ± 2.3	37.5 ± 0.6
4aa	Ph		CH_3	41.5 ± 0.6	45.0 ± 2.4
4bb	Ph		CH_3	21.7 ± 0.8	9.0 ± 0.1
4cc	CF_3		CH_3	3.1 ± 0.2	0.6 ± 0.0
4dd	CF_3		CH_3	12.3 ± 0.8	0.6 ± 0.0
4ee	CF_3		CH_3	43.6 ± 0.5	17.3 ± 0.4
4ff	CF_3		CH_3	45.8 ± 0.7	14.4 ± 0.6
4gg	PhCO		CH_3	58.9 ± 1.5	59.9 ± 4.7
4hh	PhCO		CH_3	52.7 ± 1.6	51.6 ± 5.4
4ii	PhCO		CH_3	41.1 ± 0.3	40.0 ± 3.9
4jj	PhCO		CH_3	45.9 ± 0.9	46.2 ± 2.6
4kk	PhCO		CH_3	43.3 ± 0.2	40.6 ± 0.9
4ll	PhCO		CH_3	11.0 ± 1.2	10.5 ± 0.9
4mm	PhCO		CH_3	10.8 ± 1.3	9.4 ± 2.6

[a]SH-SY5Y or H4 cells were pretreated with DMSO or compounds (50 μM salubrinal; 25 μM benzodiazepinones) for 2 h and then treated with DMSO or 7.5 μM thapsigargin for an additional 18 h. Cell viability was assessed using the CellTiter 96 AQ_{ueous} One Solution Cell Proliferation Assay. Wells containing 100 μL of DMEM but no cells were used as background, whereas wells treated with DMSO but no thapsigargin were used as positive controls. The viability (% of control) = 100 × (well value − average of background)/(average of positive control − average of background). The data were analyzed using MS Excel software. The experiments were repeated at least three times, and the data are represented as the average ± SEM.

prostate (PPC1), or mouse melanoma (SW1) tumor cell lines.[20]

Herein we describe the expansion of the structure−activity relationship (SAR) around the benzodiazepinone derivatives and evaluate their activity as inhibitors of thapsigargin-induced p38 activity and apoptosis in human neuronal cell lines. We also describe experiments that provide insight into the cellular mode of action (MOA) of these ER stress inhibitors and evaluate their druglike properties in readiness for in vivo proof-of-concept (POC) studies.

RESULTS AND DISCUSSION

Our preliminary analysis of the benzodiazepinone hits from phenotypic screening in rat neuronal cells led to the identification of several compounds that inhibit ER stress-mediated cell death through suppression of the ASK1 pathway.[20] Among the hits from screening, the 3-phenyl derivative ML037 (Figure 3) was identified and characterized as an MLPCN probe compound for this project. To determine the structural characteristics that could impart cytoprotective activity in human neuronal cell lines, we synthesized a library of new analogues (Table 1) to diversify the SAR around the benzodiazepinone core scaffold present in the screening hits. The analogues were designed to probe the structural requirements for cytoprotective potency and efficacy in human neuronal cells. We therefore synthesized a series of benzodiazepinone derivatives (Figure 3) in which substituents were varied at the 3-position (R^2 = H or Me), the 7-position (R^1 = Cl, Br, Ph, CF_3, or COPh), or the 4′-position of the 11-phenyl moiety (R^3). Our rationale for making these specific

DOI: 10.1021/cn500297v
ACS Chem. Neurosci. 2015, 6, 464−475

Scheme 1[a]

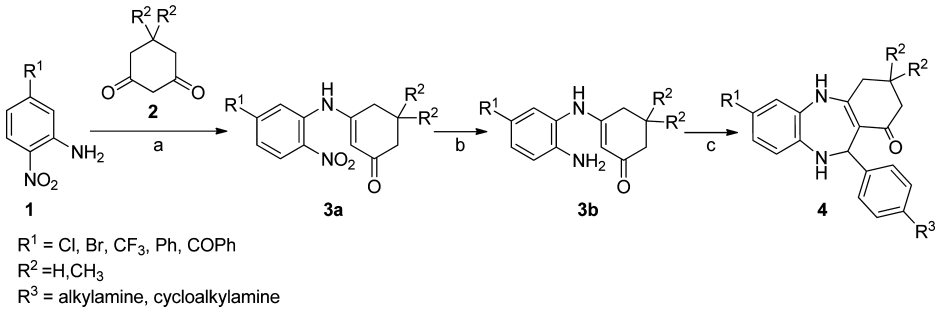

[a]Reagents and conditions: (a) **2**, PTSA, toluene, Dean−Stark trap. (b) Zn, $FeSO_4$, NH_4Cl, ethanol, water. (c) R^4CHO, $MgSO_4$, AcOH, ethanol.

modifications included removal of the phenyl group at position 3 (R^2) to eliminate a chiral center and simplify the structures. We also sought to investigate the effects of varying R^3 to determine the importance of the *N*-ethyl substituents present in ML037 (Figure 3). The analogues were synthesized using the chemistry shown in Scheme 1. Accordingly, treatment of 2-nitroaniline derivative **1** with 1,3-dione derivative **2** in benzene containing a catalytic amount of *p*-toluenesulfonic acid produces the homologous amide **3a**. Reduction of the nitro group in **3a** with zinc, ferrous sulfate and ammonium chloride produces the amine derivative **3b**. Treatment of intermediate **3b** with an aldehyde (R^4CHO = $R^3C_6H_4CHO$) in a hot solution of acetic acid in ethanol produces the desired benzodiazepinone analogues **4** in high overall yield.

The newly synthesized compounds were then tested in viability assays to determine their ability to protect against thapsigargin-induced cell death. Since ER stress is a critical component of many human neurodegenerative diseases, the benzodiazepinone derivatives were tested in two human neuronal cell lines, SH-SY5Y neuroblastoma cells and H4 glioma cells. Testing was accomplished by incubating cells for 2 h with the benzodiazepinone derivatives followed by addition of thapsigargin. Cell viability measurements were taken 18 h after thapisgargin treatment. As shown in Table 1, several compounds were found to exhibit cytoprotective effects against thapsigargin (7.5 μM) treatment. Dose−response experiments were then performed to determine the potencies (EC_{50} values, Table 2) for cytoprotective effects of those compounds initially determined to protect against ER stress in the single concentration assays. Analysis of the SAR data shown in Tables 1 and 2 revealed some interesting trends. For example, it became apparent that substitution at the 3-position (R^2) is necessary for activity since all of the analogues lacking substituents at this position (**4a**−**4i**) were inactive. In the series with R^2 = Me, all of the compounds with R^1 = Cl (**4m**−**4r**) displayed EC_{50} values for cytoprotection of >20 μM (Table 2). Interestingly, however, in the R^1 = Br series, compound **4s** was cytoprotective in H4 cells (EC_{50} ≈ 13 μM) while compound **4t** was cytoprotective in SH-SY5Y cells (EC_{50} ≈ 15 μM). In the same vein, compound **4w** in the Br series showed protective activity in H4 cells (EC_{50} ≈ 13 μM) but not in SH-SY5Y cells. On the other hand, in the series of analogues where R^1 = Ph (**4x**−**4bb**), all but one analogue (**4bb**) exhibited robust cytoprotective activity in both cell lines. Compounds **4y** and **4z** were the most potent in the R^1 = Ph series, with EC_{50} values of 9.60 and 6.85 μM, respectively, in H4 cells. Potency values declined somewhat in the R^1 = CF_3 series (**4cc**−**4ff**), although compounds **4ee** and **4ff** displayed EC_{50} values of <20 μM in both cell lines. In contrast, five compounds in the R^1 = COPh (benzophenone) series (**4gg**−**4kk**) all showed robust cytoprotective activity in both cell lines. It is notable, however, that compounds **4ll** (R^3 = OH) and **4mm** (R^4 = 3-thiophenyl) were devoid of cytoprotective activity and were therefore used as inactive controls in further experiments. Based on its overall profile in the cell viability assays, compound **4hh** (EC_{50} = 7.00 μM in SH-SY5Y cells, EC_{50} = 11.4 μM in H4 cells) was selected for additional characterization. The robust, dose-dependent cytoprotective activity of compound **4hh** is shown graphically in Figure 4. A subset of the most potent compounds was then evaluated via in vitro absorption, distribution, metabolism, and excretion (ADME) assays to determine their plasma stability,

Table 2. Potency and Efficacy of Cytoprotective Benzodiazepinone Analogues[a]

	SH-SY5Y		H4	
compd	EC_{50} ± SEM (μM)	MAX ± SEM (% viability)	EC_{50} ± SEM (μM)	MAX ± SEM (% viability)
4j	>50 ± na	41.1 ± 4.6	>50 ± na	23.3 ± 7.7
4k	>50 ± na	22.5 ± 2.7	>50 ± na	12.1 ± 2.8
4n	>50 ± na	60.4 ± 3.9	>50 ± na	22.0 ± 3.9
4o	35.62 ± 2.74	62.9 ± 7.3	20.61 ± 0.66	22.5 ± 2.3
4p	40.44 ± 2.06	69.0 ± 1.1	27.50 ± 3.32	26.0 ± 1.9
4r	>50 ± na	61.1 ± 5.0	22.25 ± 1.55	24.7 ± 2.5
4s	>50 ± na	22.3 ± 4.6	12.86 ± 0.92	60.9 ± 4.4
4t	14.57 ± 1.61	59.3 ± 6.7	>50 ± na	28.8 ± 1.8
4u	31.39 ± 0.99	69.8 ± 0.8	26.30 ± 1.34	29.9 ± 1.7
4w	>50 ± na	52.2 ± 2.4	13.11 ± 2.53	25.7 ± 3.4
4x	21.04 ± 0.26	63.4 ± 6.5	14.32 ± 0.31	44.9 ± 1.0
4y	11.42 ± 1.03	66.2 ± 5.0	9.60 ± 1.06	52.0 ± 2.2
4z	13.78 ± 3.62	64.3 ± 5.2	6.85 ± 0.98	45.6 ± 0.6
4aa	21.69 ± 2.27	64.4 ± 10.2	16.99 ± 1.41	46.9 ± 1.5
4bb	>50 ± na	67.7 ± 6.2	>50 ± na	32.9 ± 3.8
4ee	14.02 ± 0.18	71.2 ± 1.6	18.81 ± 2.77	31.3 ± 2.5
4ff	16.02 ± 0.82	78.3 ± 8.1	19.46 ± 2.15	31.1 ± 4.1
4gg	15.30 ± 1.15	87.4 ± 0.6	15.10 ± 0.67	69.9 ± 3.2
4hh	7.00 ± 0.16	84.8 ± 3.3	11.40 ± 2.26	59.5 ± 0.2
4ii	12.33 ± 1.59	70.5 ± 4.7	19.02 ± 1.28	60.9 ± 1.4
4jj	14.98 ± 0.47	71.7 ± 5.7	14.73 ± 3.52	65.6 ± 5.1
4kk	19.81 ± 2.38	71.3 ± 2.7	18.87 ± 1.30	59.6 ± 3.1

[a]EC_{50} values and percent maximal viability for analogues were obtained by treating SH-SY5Y or H4 cells with 7.5 μM thapsigargin and various concentrations of hit compounds. Cell viability was assessed using the CellTiter 96 AQ_{ueous} One Solution Cell Proliferation Assay. The results were analyzed using GraphPad Prism 5. Experiments were repeated three times, and the data are represented as the average ± SEM.

DOI: 10.1021/cn500297v
ACS Chem. Neurosci. 2015, 6, 464−475

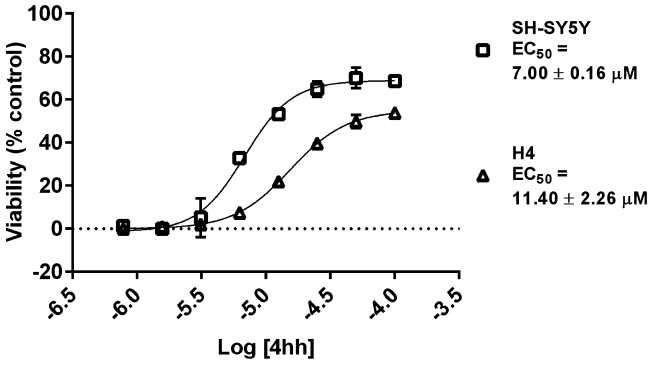

Figure 4. Compound **4hh** dose-dependently increases viability in SH-SY5Y and H4 cells. SH-SY5Y or H4 cells were pretreated with **4hh** for 2 h and then treated with 7.5 μM thapsigargin for an additional 18 h. Cell viability was assessed using the CellTiter 96 AQ_{ueous} One Solution Cell Proliferation Assay. Wells containing 100 μL of DMEM but no cells were used as background, whereas wells treated with DMSO but no thapsigargin were used as positive controls. The viability (% of control) = 100 × (well value − average of background)/(average of positive control − average of background). Experiments were repeated at least three times, and the data are represented as the average ± SEM.

microsomal stability, and permeability (Table 3). The in vitro ADME data indicate that the selected compounds are highly

Table 3. ADME Values for Selected Compounds[a]

	microsomal stability	plasma stability	PAMPA
compd	% remaining (1 h)	% remaining (3 h)	log Papp
4hh	7.9 ± 6.3	≥100	−7.33
4t	0.1 ± 0.1	≥100	N/A
4y	1.8 ± 2.1	97.9 ± 5.7	−7.12
4ee	1.8 ± 0.4	98.8 ± 3.7	−7.54
4ff	4.7 ± 1.7	≥100	−7.46
4jj	12.9 ± 1.6	≥100	−10.20

[a]Compounds with highest relative potency were analyzed for stability in mouse microsomes and plasma, as well as for BBB permeability.

stable in plasma, but have low stability in liver microsomes and may have poor blood-brain barrier (BBB) permeability as predicted by a parallel artificial membrane permeability assay (PAMPA). In addition, compound **4hh** was tested against a panel of 46 receptors, ion channels, and transporters through the NIMH Psychoactive Drug Screening Program (PDSP), and the data are included in Table S1 in the Supporting Information. No significant off-target interactions were detected.

We previously performed experiments suggesting that this series of benzodiazepinone derivatives specifically target the ASK1 signaling pathway,[20] resulting in reduced signaling from this stress kinase. Consequently, we evaluated **4hh** to determine whether it inhibited the activation of signaling effectors downstream of ASK1. As ASK1 activity results in the phosphorylation and subsequent activation of p38 MAPK and JNK, immunoblots using phospho-specific antibodies were performed on H4 cellular lysates. H4 cells pretreated with DMSO alone displayed robust phosphorylation of both p38 and JNK following 1 h of thapsigargin treatment. However, in cells pretreated with various concentrations of **4hh**, p38 and JNK activity in response to thapsigargin treatment was significantly reduced (Figure 5). Conversely, pretreatment

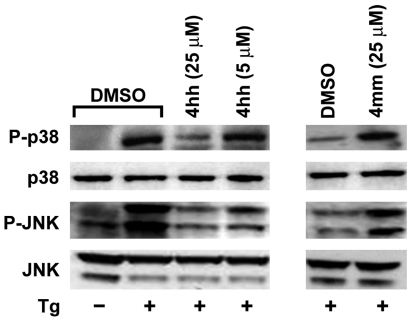

Figure 5. Benzodiazepinones inhibit thapsigargin-induced p38 MAPK and JNK activation. H4 cells were pretreated with DMSO or benzodiazepinones for 2 h and then treated with 20 μM thapsigargin for one more hour. Cell lysates were collected and analyzed by SDS-PAGE/immunoblotting. Specific antibodies for phospho-p38 MAPK, p38 MAPK, phospho-JNK, and JNK were used. **4hh** is an active benzodiazepinone, while **4mm** is inactive.

with the inactive analogue **4mm** had no effect. These data suggest that, as with the previously characterized screening hits, **4hh** inhibits thapsigargin-induced activation of the proapoptotic kinases p38 and JNK that are activated downstream of ASK1.[20]

We next investigated whether **4hh** possessed cytoprotective activity against cell death initiated in response to activators of cellular stress other than thapsigargin. The compounds tested covered a range of cell stress events, including ER stress [tunicamycin, carbobenzoxy-Leu-Leu-leucinal (MG132), or dithiothreitol (DTT)], broad kinase inhibition (staurosporine), oxidative stress [6-hydroxydopamine (6-OHDA), paraquat, or H_2O_2], and activation of the ASK1 kinase pathway [3′,4′-dichloro-3-(3,4-dichlorophenylacetyl)-2,4,6-trihydroxydeoxybenzoin (DDTD)].[21] Thus, SH-SY5Y cells were pretreated with **4hh** or the inactive analogue **4mm**, which was utilized as a negative control, and then stimulated with the various cell stress inducers. Cellular viability was quantified using the CellTiter 96 Aqueous One Solution Cell Proliferation Assay (Promega) or ATPlite (PerkinElmer). Interestingly, we found that **4hh** specifically protected against thapsigargin-induced cell death and offered no protection against other activators of cell stress (Figure 6). This specificity for thapsigargin-induced cell stress suggests that **4hh** may act upon pathways uniquely initiated through thapsigargin treatment.

Thapsigargin is a noncompetitive SERCA inhibitor that increases the cytosolic calcium concentration in cells by preventing uptake of calcium by the ER.[22] Therefore, we next examined whether **4hh** inhibited p38 activation by other compounds that disrupt calcium homeostasis. To analyze p38 activity, we utilized H4 cells expressing a CHOP-luciferase reporter system. When active, p38 MAPK upregulates the transcriptional activity of CHOP through the phosphorylation of two serine residues in the CHOP transactivation domain. H4 cells stably expressing pFR-Luc and pFA-CHOP plasmids were pretreated with DMSO, **4hh**, or the inactive analogue **4ll**. Additionally, a p38 inhibitor was used as a positive control. p38 activation was induced using the synthetic triterpenoid, 2-cyano-3,12-dioxooleana-1,9-dien-28-oic acid (CDDO), or with ionomycin, both of which have been demonstrated to increase cytoplasmic free Ca^{2+}.[14,23,24] The proteasome inhibitor MG132 was also used to stimulate p38 activity.[25] We found that treatment with **4hh** reduced p38 activation initiated by thapsigargin, CDDO-IM, or ionomycin, but had no effect on p38 activity stimulated by MG132 (Figure 7). These data

DOI: 10.1021/cn500297v
ACS Chem. Neurosci. 2015, 6, 464−475

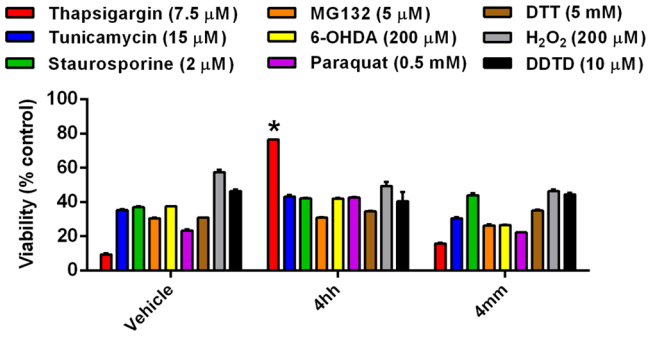

Figure 6. Compound **4hh** exhibits strong cytoprotection only with thapsigargin treatment among different p38 activating cell death inducers. SH-SY5Y cells were pretreated with DMSO or 25 μM compounds for 2 h and then treated with different inducers, including thapsigargin (7.5 μM), tunicamycin (15 μM), staurosporine (2 μM), 6-OHDA (200 μM), DTT (5 mM), and H_2O_2 (200 μM) for 18 h, and MG132 (5 μM), paraquat (0.5 mM), and DDTD (10 μM) for 48 h. Cell viability was assessed using the CellTiter 96 AQ_{ueous} One Solution Cell Proliferation Assay or ATPlite. Wells with DMSO but no inducer and no compound were used as 100% controls, and wells with DMSO and inducer but no compound were used as negative controls. The experiments were repeated at least three times, and the data are represented as the average ± SEM. Asterisk (*) shows that **4hh** exhibits very strong cytoprotective activity against thapsigargin-induced cell death whereas the inactive compound **4mm** does not.

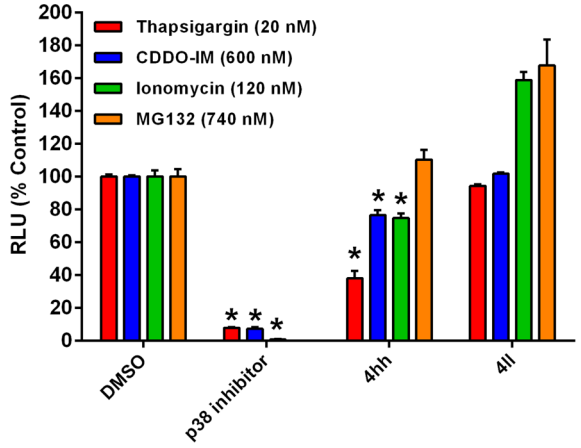

Figure 7. Active benzodiazepinone **4hh**, but not inactive compound **4ll**, inhibits calcium regulator-induced p38 MAPK activation. H4-CHOP-luciferase reporter cells were pretreated with DMSO or compounds for 1 h and then treated with thapsigargin (20 nM), CDDO-IM (600 nM), ionomycin (120 nM), or MG132 (740 nM) for an additional 18 h. The luciferase expression was assessed using the Steady-Glo luciferase assay reagent. The p38 inhibitor was used at 20 μM. The benzodiazepiones **4hh** or **4ll** (10 μM) were used with thapsigargin or CDDO-IM treatment, while concentrations of 20 and 50 μM were tested with MG132 and ionomycin treatment, respectively. Wells treated with compounds only but no inducers were used as background control correspondingly, and wells treated with inducers but no compounds were used as 100% controls. The RLU (% of control) = 100 × (well value − average of background)/(average of 100% control − average of background). The data were analyzed using MS Excel software. The experiments were repeated at least three times, and the data are represented as the average ± SEM. Statistical significance ($P < 0.05$) was determined using one-way analysis of variance. *Significance was compared with inducer treatment groups.

suggest that a potential mechanism by which **4hh** alleviates stress-induced apoptosis is through reducing the activation of stress kinases in response to calcium dysregulation.

CONCLUSIONS

Compounds that protect against ER stress have great potential to ameliorate neuronal death and dysfunction associated with neurodegenerative disorders. We previously demonstrated that benzodiazepinone derivatives have cytoprotective properties in rodent neurons treated with thapsigargin.[20] We have extended these studies by expanding the SAR in this series. Thirty nine new benzodiazepinone analogues were synthesized and tested for their ability to inhibit ER stress-mediated cell death. Of these, the most potent compound was **4hh**, which protects against thapsigargin-induced ER stress in SH-SY5Y cells with a potency of approximately 7 μM. This compound is also cytoprotective in H4 human neuronal cells and reduces the activity of the stress kinases JNK and p38 MAPK in response to thapsigargin. Additionally, **4hh** appears to specifically reduce the activation of stress kinases in response to the dysregulation of calcium homeostasis. Calcium plays a critical role in neuronal signaling and disruptions in calcium homeostasis in both the ER and mitochondria have been identified in ALS.[26] Specifically, motor neurons expressing G93A hSOD1 mutations, which have been linked to familial ALS, displayed increased calcium uptake by SERCA receptors coupled with alterations in mitochondrial calcium efflux.[27,28] In addition, some motor neurons have been demonstrated to be particularly vulnerable to alterations in calcium.[29,30] The biological characteristics of the benzodiazepinone derivatives in our study suggest that these compounds may provide the basis of a treatment for disease states where ER stress leads to neuronal death and dysfunction. Taken together, our data support the continued investigation of benzodiazepinone analogues as potential therapeutic agents for neuronal disorders that feature neuron loss in response to ER stress. It is notable that these compounds specifically inhibit stress kinase activation in response to the disruption of calcium homeostasis, an initiator of both ER stress and neuronal dysfunction.

METHODS

General Methods for the Synthesis of Benzodiazepinone Derivatives. *General Method A.* A stirred solution of the substituted 2-nitroaniline **1** (1 mmol, 1 equiv), 1,3-cyclohexanedione **2** (1.5 mmol, 1.5 equiv), 50 mL of toluene, and PTSA (0.1 mmol, 0.1 equiv) was heated at reflux using a Dean−Stark trap for 12−24 h. When the reaction was completed, as determined by HPLC-MS analysis, the reaction was cooled to room temperature. The crude reaction mixture was diluted with 100 mL of ethyl acetate and washed twice with saturated $NaHCO_3$ solution (50 mL). The organic layers were collected and dried over Na_2SO_4. The solvents were removed by rotary evaporation, and the products were isolated by flash chromatography (hexane/ethyl acetate 90:10 to 50:50 gradient) and concentrated in vacuo to provide the compound **3a** (yield 50−85%) which was determined to be >95% pure by HPLC-MS and ^1H NMR.

General Method B. To solution of compound **3a** (1 mmol, 1 equiv), ethanol (50 mL), iron sulfate heptahydrate (3 mmol, 3 equiv), water (9 mL), and ammonium chloride (8 mmol, 8 equiv) was added with efficient stirring zinc powder (3 mmol, 3 equiv). The reaction mixture was then heated for 3−12 h at 50 °C. When the reaction was completed, as determined by HPLC-MS analysis, the reaction mixture was cooled to room temperature and filtered over a pad of Celite (5g) with suction. The filter cake was washed with ethanol, and the filtrate was concentrated under reduced pressure to a residue. The residue was dissolved in CH_2Cl_2 (50 mL), and 50 mL of water was added. The

DOI: 10.1021/cn500297v
ACS Chem. Neurosci. 2015, 6, 464−475

organic layer was separated and dried over Na_2SO_4. The solvents were removed by rotary evaporation and the products were isolated by flash chromatography (hexane/ethyl acetate 90:10 to 50:50 gradient) to provide the compound **3b** (yield 90−95%) which was determined to be >95% pure by HPLC-MS and ^{1}H NMR.

General Method C. A stirred solution of compound **3b** (1 mmol, 1 equiv) in ethanol (50 mL), R^4CHO (1.1 mmol, 1.1 equiv), and $MgSO_4$ (2 mmol, 2 equiv) was heated for 12−24 h at 70 °C. When the reaction was completed, as determined by HPLC-MS analysis, the reaction was cooled to room temperature and filtered, the filtrate was removed by rotary evaporation, and the products were isolated by preparative HPLC (C-18 column eluted with MeOH containing 0.05% formic acid and water containing 0.5% formic acid, 10:90 to 100:0 gradient) to provide the final compound **4** (yield 55−78%) which was determined to be >95% pure by HPLC-MS and ^{1}H NMR.

*7-Chloro-11-(4-(diethylamino)phenyl)-2,3,4,5,10,11-hexahydro-1H-dibenzo[b,e][1,4] diazepin-1-one (**4a**).* ^{1}H NMR (400 MHz, $CDCl_3$): δ 6.87 (m, 2H), 6.70 (m, 1H), 6.44 (m, 3H), 6.21 (m, 1H), 5.81 (s, 1H), 3.23 (m, 4H), 2.70−2.60 (m, 2H), 2.40 (m, 2H), 2.08 (m, 2H), 1.07 (m, 3H). ^{13}C NMR (100 MHz, DMSO-d_6): δ 192.5, 156.0, 145.7, 138.1, 132.1, 130.4, 128.0, 122.2, 121.7, 118.7, 112.7, 110.9, 54.5, 43.5, 36.0, 31.0, 21.5, 12.5. ESI-MS *m/z* 396 $[M + H]^+$. HRMS *m/z* calcd for $C_{23}H_{27}ClN_3O$ $[M + H]^+$: 396.1837. Found: 396.1838.

*7-Chloro-11-(4-(pyrrolidin-1-yl)phenyl)-2,3,4,5,10,11-hexahydro-1H-dibenzo[b,e] [1,4]diazepin-1-one (**4b**).* ^{1}H NMR (400 MHz, DMSO-d_6): δ 8.72 (s, 1H), 6.90−6.86 (m, 3H), 6.60−6.54 (m, 2H), 6.29−6.27 (m, 2H), 6.59 (s, 1H), 3.09 (m, 4H), 2.65 (m, 2H), 2.23(m, 2H), 1.93−1.87 (m, 6H). ^{13}C NMR (100 MHz, DMSO-d_6): δ 192.5, 156.1, 145.9, 127.9, 121.6, 118.7, 118.3, 110.9, 54.7, 47.2, 35.9, 30.7, 24.8, 21.4. ESI-MS *m/z* 394 $[M + H]^+$. HRMS *m/z* calcd for $C_{23}H_{24}ClN_3O$ $[M + H]^+$: 394.1608. Found: 394.1592.

*7-Chloro-11-(4-(piperidin-1-yl)phenyl)-2,3,4,5,10,11-hexahydro-1H-dibenzo[b,e][1,4] diazepin-1-one (**4c**).* ^{1}H NMR (400 MHz, $CDCl_3$): δ 6.91 (m, 2H), 6.71 (m, 3H), 6.5−6.20 (m, 2H), 5.84 (s, 1H), 3.04 (m, 4H), 2.70−2.60 (m, 2H), 2.40 (m, 2H), 2.11 (m, 2H), 1.52 (m, 6H). ^{13}C NMR (100 MHz, $CDCl_3$): δ 194.1, 153.8, 151.7, 138.7, 136.2, 131.9, 129.4, 125.8, 123.4, 122.6, 120.9, 120.5, 119.1, 116.3, 113.9, 113.5, 57.2, 57.0, 50.6, 36.2, 32.8, 25.8, 24.1, 21.6. ESI-MS *m/z* 408 $[M + H]^+$. HRMS *m/z* calcd for $C_{24}H_{27}ClN_3O$ $[M + H]^+$: 408.1837. Found: 408.1824.

*7-Chloro-11-(4-morpholinophenyl)-2,3,4,5,10,11-hexahydro-1H-dibenzo[b,e][1,4]diazepin-1-one (**4d**).* ^{1}H NMR (400 MHz, $CDCl_3$): δ 6.94 (m, 2H), 6.68 (m, 4H), 6.50−6.30 (m, 2H), 5.85 (s, 1H), 3.80 (m, 4H), 3.04 (m, 4H), 2.75−2.60 (m, 2H), 2.41 (m, 2H), 2.06 (m, 2H). ^{13}C NMR (100 MHz, DMSO-d_6): δ 192.6, 156.1, 149.0, 138.0, 134.6, 132.2, 127.8, 122.4, 121.7, 121.5, 118.8, 114.4, 112.4, 66.0, 54.7, 48.3, 36.0, 31.1, 21.5. ESI-MS *m/z* 410 $[M + H]^+$. HRMS *m/z* calcd for $C_{23}H_{25}ClN_3O_2$ $[M + H]^+$: 410.1630. Found: 410.1609.

*7-Chloro-11-(4-(dibutylamino)phenyl)-2,3,4,5,10,11-hexahydro-1H-dibenzo[b,e][1,4] diazepin-1-one (**4e**).* ^{1}H NMR (400 MHz, $CDCl_3$): δ 6.84−6.75 (m, 3H), 6.65 (m, 1H), 6.37 (m, 3H), 5.81 (s, 1H), 3.13 (m, 4H), 2.55 (m, 2H), 2.37 (m, 2H), 2.00 (m, 2H), 1.46 (m, 2H), 1.27 (m, 2H), 0.90 (m, 6H). ^{13}C NMR (100 MHz, $CDCl_3$): δ 194.4, 155.0, 146.9, 138.8, 136.4, 132.0, 130.0, 128.0, 125.3, 123.2, 122.4, 120.7, 119.5, 113.9, 111.4, 57.0, 50.7, 36.2, 32.4, 29.4, 21.6, 20.3, 13.9. ESI-MS *m/z* 452 $[M + H]^+$. HRMS *m/z* calcd for $C_{27}H_{35}ClN_3O$ $[M + H]^+$: 452.2463. Found: 452.2453.

*7-Bromo-11-(4-(dimethylamino)phenyl)-2,3,4,5,10,11-hexahydro-1H-dibenzo[b,e][1,4] diazepin-1-one (**4f**).* ^{1}H NMR (400 MHz, $CDCl_3$): δ 6.88 (m, 4H), 6.54 (m, 2H), 6.37 (m, 3H), 6.35 (m, 1H), 6.15 (m, 1H), 5.87 (s, 1H), 2.88 (m, 6H), 2.67 (m, 2H), 2.44 (m, 2H), 2.12 (m, 2H). ^{13}C NMR (100 MHz, $CDCl_3$): δ 194.1, 153.4, 136.6, 132.2, 131.2, 127.8, 126.2, 122.9, 121.9, 114.2, 112.6, 57.0, 40.6, 36.2, 32.8, 21.6. ESI-MS *m/z* 414 $[M + H]^+$. HRMS *m/z* calcd for $C_{21}H_{23}BrN_3O$ $[M + H]^+$: 414.1001. Found: 414.0983.

*7-Bromo-11-(4-(diethylamino)phenyl)-2,3,4,5,10,11-hexahydro-1H-dibenzo[b,e] [1,4]diazepin-1-one (**4g**).* ^{1}H NMR (400 MHz, DMSO-d_6): δ 8.71 (s, 1H), 7.05 (s, 1H), 6.85−6.84 (m, 2H), 6.71 (m, 1H), 6.51 (m, 1H), 6.40 (m, 3H), 6.29 (s, 1H), 5.56 (s, 1H), 3.31−3.20 (m, 4H), 2.64 (m, 2H), 2.23 (m, 2H), 1.93 (m, 2H), 0.99−0.98 (m, 6H). ^{13}C NMR (100 MHz, DMSO-d_6): δ 192.5, 155.9, 145.7, 138.5, 132.5, 130.5, 128.0, 124.5, 121.9, 121.5, 112.7, 110.8, 109.7, 54.4, 43.5, 46.0, 30.7, 21.5, 12.4. ESI-MS *m/z* 440 $[M + H]^+$. HRMS *m/z* calcd for $C_{23}H_{26}BrN_3O$ $[M + H]^+$: 440.1259. Found: 440.1254.

*7-Bromo-11-(4-(piperidin-1-yl)phenyl)-2,3,4,5,10,11-hexahydro-1H-dibenzo[b,e][1,4] diazepin-1-one (**4h**).* ^{1}H NMR (400 MHz, $CDCl_3$): δ 6.88 (m, 3H), 6.78 (m, 1H), 6.70 (m, 2H), 6.60 (s, 1H), 6.30 (m, 1H), 5.84 (s, 1H), 3.02 (m, 4H), 2.61 (m, 2H), 2.39 (m, 2H), 2.05 (m, 2H), 1.63 (m, 6H). ^{13}C NMR (100 MHz, $CDCl_3$): δ 194.3, 154.5, 150.7, 136.7, 133.8, 132.3, 127.7, 126.2, 122.9, 122.1, 116.1, 113.7, 112.7, 57.1, 50.4, 36.2, 32.6, 25.8, 24.2, 21.6. ESI-MS *m/z* 454 $[M + H]^+$. HRMS *m/z* calcd for $C_{24}H_{27}BrN_3O$ $[M + H]^+$: 454.1315. Found: 454.1275.

*7-Bromo-11-(4-(dibutylamino)phenyl)-2,3,4,5,10,11-hexahydro-1H-dibenzo[b,e][1,4] diazepin-1-one (**4i**).* ^{1}H NMR (400 MHz, $CDCl_3$): δ 6.90−6.75 (m, 4H), 6.40 (m, 4H), 5.81 (s, 1H), 3.14 (q, *J* = 6.4 Hz, 4H), 2.63 (m, 2H), 2.40 (m, 2H), 2.05 (m, 2H), 1.47 (m, 4H), 1.29 (m, 4H), 0.92 (m, 6H). ^{13}C NMR (100 MHz, $CDCl_3$): δ 194.2, 153.8, 147.0, 136.8, 132.1, 129.7, 128.0, 126.1, 122.9, 122.0, 114.3, 112.4, 111.4, 56.9, 50.7, 36.2, 32.7, 29.4, 21.6, 20.3, 14.0. ESI-MS *m/z* 498 $[M + H]^+$. HRMS *m/z* calcd for $C_{27}H_{35}BrN_3O$ $[M + H]^+$: 498.1941. Found: 498.1932.

*11-(4-(Dimethylamino)phenyl)-7-(trifluoromethyl)-2,3,4,5,10,11-hexahydro-1H-dibenzo[b,e] [1,4]diazepin-1-one (**4j**).* ^{1}H NMR (400 MHz, DMSO-d_6): l)8.86 (s, 1H), 7.21 (s, 1H), 6.91(m, 3H), 6.73 (m, 2H), 6.50 (m, 2H), 5.64 (s, 1H), 2.75−2.74 (d, 6H), 2.66 (m, 2H), 2.25 (m, 2H), 1.94 (m, 2H). ^{13}C NMR (100 MHz, DMSO-d_6): 2192.5, 156.3, 148.6, 142.5, 131.5, 130.5, 127.7, 120.2, 118.9, 116.4, 112.6, 112.0, 54.0, 36.0, 30.5, 21.4. ESI-MS *m/z* 402 $[M + H]^+$. HRMS *m/z* calcd for $C_{22}H_{22}F_3N_3O$ $[M + H]^+$: 402.1715. Found: 402.1716.

*11-(4-(Diethylamino)phenyl)-7-(trifluoromethyl)-2,3,4,5,10,11-hexahydro-1H-dibenzo[b,e] [1,4]diazepin-1-one (**4k**).* ^{1}H NMR (400 MHz, $CDCl_3$): δ 7.00−6.85 (m, 4H), 6.57 (m, 1H), 6.45 (d, *J* = 6.4 Hz, 2H), 6.23 (s, 1H), 5.86 (s, 1H), 3.23 (q, *J* = 4.6 Hz, 4H), 2.80−2.55 (m, 2H), 2.42 (m, 2H), 2.20−2.00 (m, 2H), 1.06 (t, *J* = 4.6 Hz, 6H). ^{13}C NMR (100 MHz, $CDCl_3$): δ 194.1, 153.6, 146.5, 140.5, 130.0, 127.9, 121.2, 120.3, 114.6, 111.6, 56.6, 44.1, 36.2, 32.7, 21.7, 12.5. ESI-MS *m/z* 430 $[M + H]^+$. HRMS *m/z* calcd for $C_{24}H_{27}F_3N_3O$ $[M + H]^+$: 430.2101. Found: 430.2093.

*11-(4-(Pyrrolidin-1-yl)phenyl)-7-(trifluoromethyl)-2,3,4,5,10,11-hexahydro-1H-dibenzo[b,e] [1,4]diazepin-1-one (**4l**).* ^{1}H NMR (400 MHz, DMSO-d_6): δ 8.85 (s, 1H), 7.22 (s, 1H), 6.90 (m, 3H), 6.72 (m, 2H), 6.30 (m, 2H), 5.62 (m, 1H), 3.08 (m, 4H), 2.66 (m, 2H), 2.23 (m, 2H), 1.88 (m, 6H). ^{13}C NMR (100 MHz, DMSO-d_6): δ 192.6, 156.3, 146.0, 142.5, 130.6, 130.4, 127.8, 120.1, 118.8, 116.4, 112.6, 111.0, 54.2, 47.1, 36.0, 30.6, 24.9, 21.5. ESI-MS *m/z* 428 $[M + H]^+$. HRMS *m/z* calcd for $C_{24}H_{24}F_3N_3O$ $[M + H]^+$: 428.1871. Found: 428.1873.

*7-Chloro-11-(4-(dimethylamino)phenyl)-3,3-dimethyl-2,3,4,5,10,11-hexahydro-1H-dibenzo [b,e][1,4]diazepin-1-one (**4m**).* ^{1}H NMR (400 MHz, $CDCl_3$): δ 6.91 (m, 2H), 6.72 (m, 2H), 6.50 (m, 2H), 6.40 (m, 1H), 6.20 (s, 1H), 5.82 (d, *J* = 7.8 Hz, 1H), 2.84 (s, 6H), 2.58 (m, 1H), 2.29 (m, 3H), 1.15 (d, *J* = 7.8 Hz, 3H), 1.09 (d, *J* = 7.8 Hz, 3H). ^{13}C NMR (100 MHz, $CDCl_3$): δ 193.9, 151.7, 149.3, 136.2, 132.0, 131.5, 127.8, 125.6, 123.4, 122.6, 119.1, 113.0, 112.4, 57.3, 49.7, 46.4, 40.6, 32.4, 28.9, 27.6. ESI-MS *m/z* 396 $[M + H]^+$. HRMS *m/z* calcd for $C_{23}H_{27}ClN_3O$ $[M + H]^+$: 396.1837. Found: 396.1840.

*7-Chloro-11-(4-(diethylamino)phenyl)-3,3-dimethyl-2,3,4,5,10,11-hexahydro-1H-dibenzo [b,e][1,4]diazepin-1-one (**4n**).* ^{1}H NMR (400 MHz, $CDCl_3$): δ 6.87 (m, 2H), 6.70 (m, 1H), 6.44 (m, 3H), 6.10 (s, 1H), 5.79 (s, 1H), 3.23 (q, *J* = 6.9 Hz, 4H), 2.58 (m, 1H), 2.29 (m, 3H), 1.07 (m, 12H). ^{13}C NMR (100 MHz, $CDCl_3$): δ 194.0, 151.9, 146.7, 138.7, 136.3, 131.9, 130.3, 129.5, 128.1, 125.4, 123.2, 122.6, 120.8, 120.4, 119.2, 113.1, 111.6, 57.1, 49.7, 46.5, 44.1, 32.4, 28.9, 27.7, 12.5. ESI-MS *m/z* 424 $[M + H]^+$. HRMS *m/z* calcd for $C_{25}H_{31}ClN_3O$ $[M + H]^+$: 424.2150. Found: 424.2186.

*7-Chloro-3,3-dimethyl-11-(4-(pyrrolidin-1-yl)phenyl)-2,3,4,5,10,11-hexahydro-1H-dibenzo [b,e][1,4]diazepin-1-one (**4o**).*

DOI: 10.1021/cn500297v
ACS Chem. Neurosci. 2015, 6, 464−475

^{1}H NMR (400 MHz, $CDCl_3$): δ 6.91 (m, 2H), 6.70 (m, 2H), 6.35 (m, 3H), 6.10 (s, 1H), 5.80 (s, 1H), 3.17 (m, 4H), 2.60 (m, 1H), 2.29 (m, 3H), 1.92 (m, 4H), 1.15 (s, 3H), 1.08 (s, 3H). ^{13}C NMR (100 MHz, $CDCl_3$): δ 193.8, 151.5, 146.7, 136.3, 132.0, 130.3, 127.8, 123.4, 122.6, 119.0, 113.1, 111.4, 57.4, 49.8, 47.4, 46.5, 32.4, 29.0, 27.7, 25.4. ESI-MS m/z 422 $[M + H]^+$. HRMS m/z calcd for $C_{25}H_{29}ClN_3O$ $[M + H]^+$: 422.1994. Found: 422. 2021.

*7-Chloro-3,3-dimethyl-11-(4-(piperidin-1-yl)phenyl)-2,3,4,5,10,11-hexahydro-1H-dibenzo [b,e][1,4]diazepin-1-one (**4p**).* ^{1}H NMR (400 MHz, $CDCl_3$): δ 6.90 (m, 2H), 6.70 (m, 4H), 6.42 (m, 1H), 6.32 (m, 1H), 5.81 (s, 1H), 3.02 (m, 4H), 2.60 (m, 1H), 2.29 (m, 3H), 1.62 (m, 4H), 1.51 (m, 2H), 1.13 (s, 3H), 1.07 (s, 3H). ^{13}C NMR (100 MHz, $CDCl_3$): δ 194.1, 152.4, 150.7, 136.2, 134.2, 131.9, 127.7, 125.6, 123.4, 122.6, 119.3, 116.2, 112.6, 57.4, 50.5, 49.8, 46.3, 32.3, 28.9, 27.7, 25.8, 24.2. ESI-MS m/z 436 $[M + H]^+$. HRMS m/z calcd for $C_{26}H_{31}ClN_3O$ $[M + H]^+$: 436.2150. Found: 436.2188.

*7-Chloro-3,3-dimethyl-11-(4-morpholinophenyl)-2,3,4,5,10,11-hexahydro-1H-dibenzo[b,e] [1,4]diazepin-1-one (**4q**).* ^{1}H NMR (400 MHz, $CDCl_3$): δ 6.94 (m, 2H), 6.68 (m, 4H), 6.34 (d, J = 8.2 Hz, 1H), 6.21 (s, 1H), 5.82 (s, 1H), 3.79 (t, J = 4.1 Hz, 4H), 3.04 (t, J = 4.1 Hz, 4H), 2.60 (m, 1H), 2.29 (m, 3H), 1.15 (s, 3H), 1.08 (s, 3H). ^{13}C NMR (100 MHz, $CDCl_3$): δ 193.9, 152.0, 149.8, 136.0, 135.1, 131.9, 127.9, 125.7, 123.4, 122.5, 119.2, 115.4, 112.6, 66.9, 57.3, 49.7, 49.2, 46.4, 32.4, 28.8, 27.7. ESI-MS m/z 438 $[M + H]^+$. HRMS m/z calcd for $C_{25}H_{29}ClN_3O_2$ $[M + H]^+$: 438.1943. Found: 438.1956.

*7-Chloro-11-(4-(dibutylamino)phenyl)-3,3-dimethyl-2,3,4,5,10,11-hexahydro-1H-dibenzo [b,e][1,4]diazepin-1-one (**4r**).* ^{1}H NMR (400 MHz, $CDCl_3$): δ 6.87 (m, 2H), 6.75 (m, 1H), 6.70 (m, 1H), 6.39 (m, 4H), 5.80 (s, 1H), 4.36 (s, 1H), 3.14 (m, 4H), 2.55 (m, 1H), 2.29 (m, 3H), 1.46 (m, 4H), 1.28 (m, 4H), 1.14 (s, 3H), 1.09 (s, 3H), 0.92 (m, 6H). ^{13}C NMR (100 MHz, $CDCl_3$): δ 194.0, 152.0, 147.0, 136.4, 131.9, 130.0, 127.9, 125.3, 123.2, 122.5, 119.2, 113.1, 111.4, 57.2, 50.7, 49.8, 46.3, 32.3, 29.4, 28.9, 27.8, 20.3, 14.0. ESI-MS m/z 480 $[M + H]^+$. HRMS m/z calcd for $C_{29}H_{39}ClN_3O$ $[M + H]^+$: 480.2776. Found: 480.2795.

*7-Bromo-11-(4-(dimethylamino)phenyl)-3,3-dimethyl-2,3,4,5,10,11-hexahydro-1H-dibenzo [b,e][1,4]diazepin-1-one (**4s**).* ^{1}H NMR (400 MHz, DMSO-d_6): δ 8.63 (s, 1H), 7.01 (m, 1H), 6.83 (d, J = 8.7 Hz, 2H), 6.65 (m, 1H), 6.42 (m, 3H), 6.20 (m, 1H), 5.51 (d, J = 5.5 Hz, 1H), 2.71 (s, 6H), 2.46 (m, 3H), 2.07 (m, 1H), 1.01 (s, 3H), 0.97 (s, 3H). ^{13}C NMR (100 MHz, DMSO-d_6): δ 192.3, 153.9, 148.6, 138.4, 132.7, 131.8, 127.8, 124.4, 122.0, 121.5, 111.8, 111.6, 109.8, 54.9, 49.4, 43.9, 31.8, 28.6, 27.2. ESI-MS m/z 442 $[M + H]^+$. HRMS m/z calcd for $C_{23}H_{27}BrN_3O$ $[M + H]^+$: 442.1314. Found: 442.1298.

*7-Bromo-3,3-dimethyl-11-(4-(pyrrolidin-1-yl)phenyl)-2,3,4,5,10,11-hexahydro-1H-dibenzo [b,e][1,4]diazepin-1-one (**4t**).* ^{1}H NMR (400 MHz, $CDCl_3$): δ 6.84 (m, 4H), 6.34 (m, 3H), 6.10 (s, 1H), 5.80 (d, 1H), 3.17 (t, J = 4.6 Hz, 4H), 2.58 (m, 1H), 2.29 (m, 3H), 1.92 (m, 4H), 1.15 (s, 3H), 1.08 (s, 3H). ^{13}C NMR (100 MHz, $CDCl_3$): δ 193.8, 151.6, 146.7, 136.7, 132.3, 130.3, 127.9, 126.2, 122.8, 121.9, 113.2, 112.6, 111.4, 57.3, 49.7, 47.4, 46.4, 32.4, 28.8, 27.7, 25.3. ESI-MS m/z 468 $[M + H]^+$. HRMS m/z calcd for $C_{25}H_{29}BrN_3O$ $[M + H]^+$: 468.1471. Found: 468.1464.

*7-Bromo-3,3-dimethyl-11-(4-(piperidin-1-yl)phenyl)-2,3,4,5,10,11-hexahydro-1H-dibenzo [b,e][1,4]diazepin-1-one (**4u**).* ^{1}H NMR (400 MHz, $CDCl_3$): δ 6.90 (m, 2H), 6.86 (s, 1H), 6.78 (m, 1H), 6.70 (m, 2H), 6.28 (d, J = 8.2 Hz, 2H), 6.20 (s, 1H), 5.82 (s, 1H), 3.03 (t, J = 5.5 Hz, 4H), 2.58 (m, 1H), 2.29 (m, 3H), 1.63 (m, 4H), 1.52 (m, 2H), 1.15 (s, 3H), 1.08 (s, 3H). ^{13}C NMR (100 MHz, $CDCl_3$): δ 193.9, 152.1, 136.5, 132.3, 127.7, 126.3, 122.9, 121.9, 116.4, 112.7, 57.2, 50.4, 49.6, 46.4, 32.3, 28.9, 27.7, 25.8, 24.2. ESI-MS m/z 482 $[M + H]^+$. HRMS m/z calcd for $C_{26}H_{31}BrN_3O$ $[M + H]^+$: 482.1628. Found: 482.1622.

*7-Bromo-3,3-dimethyl-11-(4-morpholinophenyl)-2,3,4,5,10,11-hexahydro-1H-dibenzo [b,e][1,4]diazepin-1-one (**4v**).* ^{1}H NMR (400 MHz, $CDCl_3$): δ 6.94 (m, 3H), 6.80 (m, 2H), 6.68 (m, 2H), 6.31 (m, 1H), 6.16 (m, 1H), 5.80 (m, 1H), 3.78 (m, 4H), 3.03 (m, 4H), 2.59 (m, 1H), 2.25 (m, 3H), 1.15 (s, 3H), 1.08 (s, 3H). ^{13}C NMR (100 MHz, $CDCl_3$): δ 193.9, 151.8, 149.7, 136.5, 135.0, 132.3, 127.9, 126.3, 122.9, 122.0, 115.5, 112.8, 66.9, 57.2, 49.7, 49.2, 46.5, 32.4, 28.9, 27.7. ESI-MS m/z 484 $[M + H]$+. HRMS m/z calcd for $C_{25}H_{29}BrN_3O_2$ $[M + H]^+$: 484.1421. Found: 484.1410.

*7-Bromo-11-(4-(dibutylamino)phenyl)-3,3-dimethyl-2,3,4,5,10,11-hexahydro-1H-dibenzo [b,e][1,4]diazepin-1-one (**4w**).* ^{1}H NMR (400 MHz, $CDCl_3$): δ 6.86 (m, 3H), 6.80 (m, 1H), 6.38 (m, 3H), 5.80 (s, 1H), 3.13 (t, J = 7.8 Hz, 4H), 2.52 (m, 1H), 2.29 (m, 3H), 1.46 (m, 4H), 1.27 (m, 4H), 1.12 (s, 3H), 1.07 (s, 3H), 0.91 (t, J = 7.3 Hz, 6H). ^{13}C NMR (100 MHz, $CDCl_3$): δ 194.0, 151.2, 147.0, 136.8, 132.2, 130.0, 127.9, 126.1, 122.9, 122.1, 113.0, 112.4, 111.4, 57.2, 50.7, 49.8, 46.2, 32.3, 29.4, 28.9, 27.8, 20.3, 14.0. ESI-MS m/z 526 $[M + H]^+$. HRMS m/z calcd for $C_{29}H_{39}BrN_3O$ $[M + H]^+$: 526.2255. Found: 526.2249.

*11-(4-(Dimethylamino)phenyl)-3,3-dimethyl-7-phenyl-2,3,4,5,10,11-hexahydro-1H-dibenzo [b,e][1,4]diazepin-1-one (**4x**).* ^{1}H NMR (400 MHz, $CDCl_3$): δ 7.50 (m, 2H), 7.40 (m, 2H), 7.27 (m, 1H), 6.97 (m, 4H), 6.65 (m, 3H), 5.86 (m, 1H), 2.82 (s, 6H), 2.62 (m, 1H), 2.30 (m, 3H), 1.17 (s, 3H), 1.10 (s, 3H). ^{13}C NMR (100 MHz, $CDCl_3$): δ 193.8, 152.1, 140.1, 136.9, 133.9, 131.0, 128.8, 127.9, 126.7, 126.4, 122.4, 122.0, 118.1, 112.4, 99.8, 57.3, 49.8, 46.7, 40.6, 32.3, 28.9, 27.7. ESI-MS m/z 438 $[M + H]^+$. HRMS m/z calcd for $C_{29}H_{31}N_3ONa$ $[M + Na]^+$: 460.2359. Found: 460.2360.

*11-(4-(Diethylamino)phenyl)-3,3-dimethyl-7-phenyl-2,3,4,5,10,11-hexahydro-1H-dibenzo [b,e][1,4]diazepin-1-one (**4y**).* ^{1}H NMR (400 MHz, $CDCl_3$): δ 7.48 (m, 2H), 7.38 (m, 2H), 7.27 (m, 1H), 7.00 (d, 1H), 6.91 (m, 3H)), 6.55 (m, 1H), 6.45 (d, J = 7.8 Hz, 2H), 6.30 (m, 1H), 5.85 (s, 1H), 3.21 (q, J = 6.0 Hz, 4H), 2.62 (m, 1H), 2.31 (m, 3H), 1.07 (m, 12H). ^{13}C NMR (100 MHz, $CDCl_3$): δ 193.8, 152.1, 140.2, 137.0, 133.8, 131.0, 128.6, 128.0, 126.9, 126.3, 126.3, 122.3, 122.0, 118.1, 112.8, 111.7, 57.2, 49.7, 46.7, 44.1, 32.2, 28.9, 27.6, 12.6. ESI-MS m/z 466 $[M + H]^+$. HRMS m/z calcd for $C_{31}H_{36}N_3O$ $[M + H]^+$: 466.2853. Found: 466.2839.

*3,3-Dimethyl-7-phenyl-11-(4-(pyrrolidin-1-yl)phenyl)-2,3,4,5,10,11-hexahydro-1H-dibenzo [b,e][1,4]diazepin-1-one (**4z**).* ^{1}H NMR (400 MHz $CDCl_3$): δ 7.85 (m, 2H), 7.37 (m, 2H), 7.27 (m, 1H), 6.98 (m, 5H), 6.55 (m, 1H), 6.35 (m, 1H), 5.87 (m, 1H), 3.16 (m, 4H), 2.65 (d, 1H), 2.32 (m, 3H), 1.91 (m, 3H), 1.17 (s, 3H), 1.10 (s, 3H). ^{13}C NMR (100 MHz, $CDCl_3$): δ 193.7, 152.0, 146.6, 140.3, 137.1, 134.5, 131.0, 128.7, 127.9, 126.3, 122.3, 121.9, 118.1, 111.2, 57.4, 49.7, 47.4, 46.6, 32.4, 29.1, 27.7, 25.3. ESI-MS m/z 464 $[M + H]^+$. HRMS m/z calcd for $C_{31}H_{34}N_3O$ $[M + H]^+$: 464.2696. Found: 464.2678.

*3,3-Dimethyl-11-(4-morpholinophenyl)-7-phenyl-2,3,4,5,10,11-hexahydro-1H-dibenzo [b,e][1,4]diazepin-1-one (**4aa**).* ^{1}H NMR (400 MHz $CDCl_3$): δ 7.48 (m, 2H), 7.40 (m, 2H), 7.27 (m, 1H), 7.00 (m, 4H), 6.68 (m, 2H), 6.55 (m, 1H), 6.30 (s, 1H), 5.89 (d, 1H), 3.79 (m, 4H), 3.03 (m, 4H), 2.65 (d, 1H), 2.32 (m, 3H), 1.91 (m, 3H), 1.18 (s, 3H), 1.10 (s, 3H). ^{13}C NMR (100 MHz, $CDCl_3$): δ 193.9, 152.3, 149.6, 140.0, 136.6, 135.7, 134.1, 130.8, 128.6, 127.9, 127.0, 126.4, 122.5, 121.9, 118.0, 115.5, 112.3, 66.9, 57.2, 49.7, 49.2, 46.7, 32.3, 29.0, 27.7. ESI-MS m/z 480 $[M + H]^+$. HRMS m/z calcd for $C_{31}H_{34}N_3O$ $[M + H]^+$: 480.2646. Found: 480.2614.

*11-(4-(Dibutylamino)phenyl)-3,3-dimethyl-7-phenyl-2,3,4,5,10,11-hexahydro-1H-dibenzo [b,e][1,4]diazepin-1-one (**4bb**).* ^{1}H NMR (400 MHz, $CDCl_3$): δ 7.48 (m, 2H), 7.38 (m, 2H), 7.27 (m, 1H), 7.05 (m, 1H), 6.92 (m, 2H), 6.56 (d, J = 8.2 Hz, 1H), 6.39 (d, J = 8.7 Hz, 2H), 6.28 (s, 1H), 5.84 (s, 1H), 3.12 (t, J = 8.1 Hz, 4H), 2.62 (m, 1H), 2.29 (m, 3H), 1.45 (m, 4H), 1.26 (m, 4H), 1.16 (s, 3H), 1.10 (s, 3H), 0.89 (m, 6H). ^{13}C NMR (100 MHz, $CDCl_3$): δ 193.8, 152.0, 146.9, 140.2, 137.1, 133.7, 130.8, 130.6, 128.7, 128.0, 126.7, 126.3, 122.3, 122.0, 118.1, 112.9, 111.4, 57.2, 50.7, 49.7, 46.7, 32.3, 29.3, 28.9, 27.7, 20.3, 14.0. ESI-MS m/z 522 $[M + H]^+$. HRMS m/z calcd for $C_{35}H_{44}N_3O$ $[M + H]^+$: 522.3479. Found: 522.3464.

*11-(4-(Dimethylamino)phenyl)-3,3-dimethyl-7-(trifluoromethyl)-2,3,4,5,10,11-hexahydro-1H-dibenzo[b,e][1,4]diazepin-1-one (**4cc**).* ^{1}H NMR (400 MHz, $CDCl_3$): δ 6.95 (m, 4H), 6.52 (m, 3H), 6.35 (s, 1H), 5.87 (s, 1H), 2.83 (s, 6H), 2.60 (m, 1H), 2.31 (m, 3H), 1.15 (s, 3H), 1.08 (s, 3H). ^{13}C NMR (100 MHz, $CDCl_3$): δ 194.0, 152.0, 149.2, 140.4, 131.4, 130.3, 127.7, 121.1, 120.3, 116.6, 113.0, 112.4,

DOI: 10.1021/cn500297v
ACS Chem. Neurosci. 2015, 6, 464−475

112.3, 57.0, 49.7, 46.2, 40.5, 32.4, 29.0, 27.4. ESI-MS m/z 430 $[M + H]^+$. HRMS m/z calcd for $C_{24}H_{27}F_3N_3O$ $[M + H]^+$: 430.2101. Found: 430.2083.

*11-(4-(Diethylamino)phenyl)-3,3-dimethyl-7-(trifluoromethyl)-2,3,4,5,10,11-hexahydro-1H-dibenzo[b,e][1,4]diazepin-1-one (**4dd**).* ^1H NMR (400 MHz, $CDCl_3$): δ 6.97 (s, 2H), 6.89 (d, J = 8.7 Hz, 2H), 6.52 (d, J = 8.7 Hz, 1H), 6.44 (d, J = 8.7 Hz, 2H), 6.34 (s, 1H), 5.84 (s, 1H), 3.22 (q, J = 7.4 Hz, 4H), 2.62 (m, 1H), 2.31 (m, 3H), 1.08 (m, 12H). ^{13}C NMR (100 MHz, $CDCl_3$): δ 193.9, 151.9, 146.6, 140.6, 130.1, 127.9, 121.2, 120.3, 116.5, 113.2, 111.6, 56.8, 49.7, 46.4, 44.2, 32.5, 29.0, 27.7, 12.6. ESI-MS m/z 458 $[M + H]^+$. HRMS m/z calcd for $C_{26}H_{31}F_3N_3O$ $[M + H]^+$: 458.2414. Found: 458.2366.

*3,3-Dimethyl-11-(4-(pyrrolidin-1-yl)phenyl)-7-(trifluoromethyl)-2,3,4,5,10,11-hexahydro-1H-dibenzo[b,e][1,4]diazepin-1-one (**4ee**).* ^1H NMR (400 MHz, $CDCl_3$): δ 6.95 (m, 4H), 6.54 (m, 1H), 6.35 (m, 3H), 5.86 (s, 1H), 3.17 (m, 4H), 2.59 (m, 1H), 2.30 (m, 3H), 1.92 (m, 4H), 1.16 (s, 3H), 1.08 (s, 3H). ^{13}C NMR (100 MHz, $CDCl_3$): δ 193.8, 152.0, 146.7, 140.7, 130.4, 130.3, 127.8, 121.2, 120.3, 116.7, 113.1, 111.4, 57.2, 49.7, 47.5, 46.4, 32.2, 29.0, 27.7, 25.4. ESI-MS m/z 456 $[M + H]^+$. HRMS m/z calcd for $C_{26}H_{29}F_3N_3O$ $[M + H]^+$: 456.2257. Found: 456.2237.

*3,3-Dimethyl-11-(4-(piperidin-1-yl)phenyl)-7-(trifluoromethyl)-2,3,4,5,10,11-hexahydro-1H-dibenzo[b,e][1,4]diazepin-1-one (**4ff**).* ^1H NMR (400 MHz, $CDCl_3$): δ 6.94 (m, 4H), 6.72 (m, 2H), 6.50 (m, 1H), 6.30 (m, 1H), 5.87 (d, J = 4.6 Hz, 1H), 3.03 (m, 4H), 2.60 (m, 1H), 2.28 (m, 3H), 1.63 (m, 6H), 1.15 (s, 3H), 1.08 (s, 3H). ^{13}C NMR (100 MHz, $CDCl_3$): δ 193.9, 152.0, 150.7, 140.5, 134.0, 130.3, 127.6, 121.2, 120.4, 116.6, 116.2, 112.8, 57.0, 50.5, 49.7, 46.4, 32.4, 28.9, 27.5, 25.8, 24.1. ESI-MS m/z 470 $[M + H]^+$. HRMS m/z calcd for $C_{27}H_{31}F_3N_3O$ $[M + H]^+$: 470.2414. Found: 470.2403.

*7-Benzoyl-11-(4-(dimethylamino)phenyl)-3,3-dimethyl-2,3,4,5,10,11-hexahydro-1H-dibenzo[b,e][1,4]diazepin-1-one (**4gg**).* ^1H NMR (400 MHz, DMSO-d_6): δ 8.81 (s, 1H), 7.53 (s, 3H), 7.46 (m, 2H), 7.03 (m, 1H), 6.90 (m, 3H), 6.62 (m, 1H), 6.46 (m, 2H), 5.61 (m, 1H), 2.71 (s, 6H), 2.46 (m, 2H), 2.15 (m, 1H), 2.00 (m, 1H), 1.01 (s, 3H), 0.95 (s, 3H). ^{13}C NMR (100 MHz, DMSO-d_6): δ 194.3, 192.8, 155.1, 149.4, 144.6, 138.9, 132.1, 130.4, 129.6, 129.0, 128.2, 127.8, 125.8, 123.0, 119.9, 112.6, 111.9, 55.0, 50.0, 44.2, 32.3, 29.5, 27.6. ESI-MS m/z 466 $[M + H]^+$. HRMS m/z calcd for $C_{30}H_{32}N_3O_2$ $[M + H]^+$: 466.2489. Found: 466.2472.

*7-Benzoyl-11-(4-(diethylamino)phenyl)-3,3-dimethyl-2,3,4,5,10,11-hexahydro-1H-dibenzo[b,e][1,4]diazepin-1-one (**4hh**).* ^1H NMR (400 MHz, $CDCl_3$): δ 7.70 (d, J = 6.9 Hz, 2H), 7.51 (m, 1H), 7.45 (m, 2H), 7.18 (m, 1H), 6.95 (d, J = 8.7 Hz, 2H), 6.70 (s, 1H), 6.52 (d, J = 8.2 Hz, 1H), 6.45 (d, J = 8.7 Hz, 2H), 5.88 (s, 1H), 3.23 (q, J = 6.9 Hz, 4H), 2.60 (m, 1H), 2.29 (m, 3H), 1.07 (m, 12H). ^{13}C NMR (100 MHz, $CDCl_3$): δ 195.3, 193.9, 152.3, 146.6, 142.5, 138.4, 131.6, 129.5, 129.3, 128.2, 127.9, 127.0, 121.9, 119.9, 112.8, 111.7, 56.6, 49.7, 46.2, 44.2, 32.2, 29.0, 27.5, 12.6. ESI-MS m/z 494 $[M + H]^+$. HRMS m/z calcd for $C_{32}H_{36}N_3O_2$ $[M + H]^+$: 494.2802. Found: 494.2725.

*7-Benzoyl-3,3-dimethyl-11-(4-(pyrrolidin-1-yl)phenyl)-2,3,4,5,10,11-hexahydro-1H-dibenzo[b,e][1,4]diazepin-1-one (**4ii**).* ^1H NMR (400 MHz, $CDCl_3$): δ 7.70 (m, 2H), 7.60−7.40 (m, 3H), 7.18 (m, 1H), 6.97 (m, 2H), 6.60−6.30 (m, 4H), 5.89 (s, 1H), 3.17 (m, 4H), 2.60 (m, 1H), 2.30 (m, 3H), 1.92 (m, 4H), 1.14 (s, 3H), 1.06 (s, 3H). ^{13}C NMR (100 MHz, $CDCl_3$): δ 193.7, 192.0, 154.5, 151.7 146.0, 144.2, 138.3, 131.0, 129.8, 129.3, 128.8, 128.5, 128.3, 122.3, 119.4, 111.3, 111.0, 54.5, 49.5, 47.3, 47.1, 43.2, 31.7, 28.8, 27.1, 24.7. ESI-MS m/z 492 $[M + H]^+$. HRMS m/z calcd for $C_{32}H_{34}N_3O_2$ $[M + H]^+$: 492.2646. Found: 492.2631.

*7-Benzoyl-3,3-dimethyl-11-(4-(piperidin-1-yl)phenyl)-2,3,4,5,10,11-hexahydro-1H-dibenzo[b,e][1,4]diazepin-1-one (**4jj**).* ^1H NMR (400 MHz, $CDCl_3$): δ 7.69 (m, 2H), 7.60−7.40 (m, 3H), 7.18 (m, 1H), 6.98 (m, 2H), 6.72 (m, 2H), 6.52 (m, 1H), 6.45 (s, 1H), 5.90 (s, 1H), 3.04 (m, 4H), 2.60 (m, 1H), 2.30 (m, 3H), 1.63 (m, 6H), 1.14 (s, 3H), 1.06 (s, 3H). ^{13}C NMR (100 MHz, $CDCl_3$): δ 195.0, 193.9, 152.3, 142.6, 138.4, 134.3, 131.7, 130.0, 129.5, 128.2, 127.5, 126.8, 121.8, 120.0, 116.3, 112.6, 56.7, 50.4, 49.6, 46.2, 32.2, 29.1, 27.5, 25.7, 24.1. ESI-MS m/z 506 $[M + H]^+$. HRMS m/z calcd for $C_{33}H_{35}N_3O_2$ $[M + H]^+$: 506.2802. Found: 506.2793.

*7-Benzoyl-3,3-dimethyl-11-(4-morpholinophenyl)-2,3,4,5,10,11-hexahydro-1H-dibenzo[b,e] [1,4]diazepin-1-one (**4kk**).* ^1H NMR (400 MHz, $CDCl_3$): δ 7.69 (d, J = 7.3 Hz, 2H), 7.52 (m, 1H), 7.46 (m, 2H), 7.15 (m, 1H), 7.04 (d, J = 6.8 Hz, 2H), 6.76 (s, 1H), 6.71 (d, J = 6.8 Hz, 2H), 6.50 (m, 1H), 5.93 (s, 1H), 3.78 (m, 4H), 3.05 (m, 4H), 2.59 (m, 1H), 2.31 (m, 3H), 1.13 (s, 3H), 1.04 (s, 3H). ^{13}C NMR (100 MHz, $CDCl_3$): δ 195.4, 193.9, 152.9, 149.7, 142.3, 138.2, 135.3, 131.8, 130.1, 129.5, 128.2, 127.8, 127.1, 122.0, 119.9, 115.5, 112.3, 66.9, 56.6, 49.7, 49.2, 46.2, 32.2, 29.1, 27.4. ESI-MS m/z 508 $[M + H]^+$. HRMS m/z calcd for $C_{32}H_{34}N_3O_3$ $[M + H]^+$: 508.2595. Found: 508.2579.

*7-Benzoyl-11-(4-hydroxyphenyl)-3,3-dimethyl-2,3,4,5,10,11-hexahydro-1H-dibenzo[b,e] [1,4]diazepin-1-one (**4ll**).* ^1H NMR (400 MHz, DMSO-d_6): δ 8.86 (s, 1H), 7.54−7.46 (m, 5H), 7.08 (m, 1H), 6.92−6.86 (m, 3H), 6.62 (m, 1H), 6.48 (m, 2H), 5.62 (s, 1H), 2.49 (s, 2H), 2.18−2.00 (m, 2H), 1.00 (s, 3H), 0.94 (s, 3H). ^{13}C NMR (100 MHz, DMSO-d_6): δ 193.7, 192.2, 155.5, 154.6, 143.7, 138.3, 134.9, 131.5, 129.8, 129.0, 128.3, 127.9, 127.3, 125.2, 122.3, 119.4, 114.7, 111.1, 54.5, 49.3, 43.8, 31.7, 28.7, 27.2. ESI-MS m/z 439 $[M + H]^+$. HRMS m/z calcd for $C_{28}H_{26}N_2O_3$ $[M + H]^+$: 439.1943. Found: 439.1942.

*7-Benzoyl-3,3-dimethyl-11-(thiophen-3-yl)-2,3,4,5,10,11-hexahydro-1H-dibenzo[b,e] [1,4]diazepin-1-one (**4mm**).* ^1H NMR (400 MHz, DMSO-d_6): δ 8.94 (s, 1H), 7.54−7.42 (m, 5H), 7.21 (m, 1H), 7.00−6.84 (m, 4H), 6.66 (m, 1H), 6.40 (m, 1H), 5.60 (s, 1H), 2.39 (s, 2H), 2.18−2.00 (m, 2H), 0.98 (s, 3H), 0.94 (s, 3H). ^{13}C NMR (100 MHz, DMSO-d_6): δ 194.4, 192.5, 154.0, 145.5, 138.2, 132.0, 130.4, 129.1, 128.2, 127.4, 125.8, 122.3, 122.0, 120.5, 119.7, 112.8, 51.6, 49.0, 43.8, 28.4, 27.5. ESI-MS m/z 429 $[M + H]^+$. HRMS m/z calcd for $C_{26}H_{24}N_2O_2S$ $[M + H]^+$: 429.1558. Found: 429.1557.

Cell Culture. SH-SY5Y cells (ATCC, CRL-2266) were maintained in DMEM/F12 (1:1, Life Technologies, 11330-032) supplemented with 10% FBS (Hyclone, SH30396.03), 100 μg/mL streptomycin, 100 IU penicillin (Life Technologies, 15140-122), and 2 mM L-glutamine (Omega, GS-60). H4 cells (ATCC, HTB-148) were maintained in DMEM (Cellgro, 15−013-CV) supplemented with 10% FBS, 100 μg/mL streptomycin, 100 IU penicillin, and 2 mM L-glutamine. The H4-CHOP-luciferase reporter cell line was maintained in DMEM supplemented with 10% FBS, 100 μg/mL streptomycin, 100 IU penicillin, 2 mM L-glutamine, 250 μg/mL Geneticin (Gibco, 10131), and 1 μg/mL Purimycin (Sigma-Aldrich, P8833). All cell lines were incubated at 37 °C with 5% CO_2.

Cell Viability Assay. *Thapsigargin as Stressor.* SH-SY5Y or H4 cells were plated in 96-well plates (Costar, 3596) with a density of 4×10^4 or 2.5×10^3 cells per well in 90 μL of phenol red-free DMEM (Cellgro, 17-205-CV) containing 2% FBS, 100 μg/mL streptomycin, 100 IU penicillin, and 2 mM L-glutamine. The plates were incubated overnight at 37 °C with 5% CO_2. The test compounds (5 μL in 10% DMSO) were added to wells to achieve a final concentration of 25 μM for screening or concentrations in dose−response experiments. Salubrinal (EMD Millipore, in 5 μL in 10% DMSO) was added to obtain a final concentration of 50 μM, whereas 5 μL of 10% DMSO was used as control. After a 2 h incubation, thapsigargin (Calbiochem, 5 μL in 10% DMSO) was added to each well to give a final concentration of 7.5 μM and, 5 μL of 10% DMSO was added to no-compound and no-thapsigargin wells as control. The plates were incubated at 37 °C for an additional 18 h. Cell viability was assessed by using the CellTiter 96 AQ_{neous} One Solution Cell Proliferation Assay (Promega, G3580). The plates were recorded using a BMG POLARstar Omega (BMG Labtech) multimode plate reader in absorbance mode. The absorbance was measured at 490 nm. Wells containing 100 μL of DMEM but no cells were used as background, whereas wells treated with DMSO but no thapsigargin were used as positive controls. The viability (% of control) = 100 × (well value − average of background)/(average of positive control − average of background). The data were analyzed by using EXCEL software for screening and GraphPad Prism 5 for dose−response results. The

DOI: 10.1021/cn500297v
ACS Chem. Neurosci. 2015, 6, 464−475

experiments were replicated at least three times, and are presented as the average ± SEM.

Other Stressors. SH-SY5Y cells and 96-well plates were used when treating cells with tunicamycin (Sigma-Aldrich, T7765, 15 μM), staurosporine (EMD Millipore, 569396, 2 μM), 6-hydroxydopamine hydrochloride (6-OHDA, Sigma-Aldrich, H4381, 200 μM), or H_2O_2 (Fisher Scientific, H323, 200 μM). The protocol was the same as that for thapsigargin treatment.

SH-SY5Y cells and 96-well plates were also used when treating cells with MG132 (EMD Millipore, 474790, 5 μM), paraquat dichloride (Sigma-Aldrich, 36541, 0.5 mM), or 3′,4′-dichloro-3-(3,4-dichlorophenylacetyl)-2,4,6-trihydroxydeoxybenzoin (DDTD,[21] 10 μM). The protocol was the same as that for thapsigargin treatment except for exposing cells to these cell death inducers for 48 h.

However, for dithiothreitol (Sigma-Aldrich, D0632) treatment, SH-SY5Y cells (10^4 cells/well) and solid white 384-well plates (Greiner Bio-one, 781080) were used by adjusting all the volumes used in the thapsigargin protocol to 1/4. The plates were assessed by using ATPlite (PerkinElmer Life Sciences, 6016941) and read on a BMG POLARstar Omega plate reader in luminescence mode. The experiments were repeated at least three times, and the data are presented as the average ± SEM.

Immunoblotting. H4 cells in phenol red-free DMEM containing 2% FBS, 100 μg/mL streptomycin, 100 IU penicillin, and 2 mM L-glutamine were seeded at a density of 2.5×10^6 in 10 cm dishes. After overnight incubation, the culture media were changed to serum-free DMEM. Following 2 h starvation, cells were pretreated with DMSO or compounds (25 μM and 5 μM) for 2 h and then exposed to 20 μM thapsigargin for an additional hour. Cells were collected in ice-cold PBS and lysed with RIPA buffer (Sigma-Aldrich, R0278) supplemented with a protease inhibitor (Roche Applied Science, 04693124001) and a phosphatase inhibitor (Roche Applied Science, 04906845001). The cell lysates were centrifuged, and supernatants were recovered. The protein concentrations were determined by using the BCA Protein Assay Kit (Pierce, 23225). Subsequently, 50 μg of cell extract was analyzed by SDS-PAGE/immunoblotting. Here, NuPAGE 4−12% Bis-Tris Gels (Life Technologies, NP0321) and iBlot Transfer Stack, PVDF Regular (Life Technologies, IB401001) were used. The primary antibodies included anti-phospho-p38 MAPK antibody (Cell Signaling Technology, 9211), anti-p38 MAPK (Cell Signaling Technology, 9212), anti-phospho-JNK antibody (Promega, V7931), and anti-JNK antibody (Santa Cruz Biotechnology, sc-7345). HRP conjugated goat anti-rabbit IgG (Thermo Scientific, 31466) and HRP-linked anti-mouse IgG (Cell Signaling Technology, 7076) were used as secondary antibodies. To develop the Western blots, ECL Detection Reagents (GE Healthcare Life Sciences, RPN2106) were used.

Activity of p38 MAPK Pathway. H4-CHOP-luciferase reporter cells [stably expressing pFR-Luc and pFA-CHOP plasmids (Agilent)] were plated in 384-well white LIA-plate (Greiner # 781080) at a cell density of 1000 cells/well in DMEM containing 10% FBS, 100 μg/mL streptomycin, 100 IU penicillin, and 2 mM L-glutamine. After 24 h incubation at 37 °C, 5% CO_2, the media in each well was replaced with 45 μL of assay media (phenol red-free DMEM containing 2% FBS, 100 μg/mL streptomycin, 100 IU penicillin, and 2 mM L-glutamine). Either 2.5 μL of test compounds or p38 MAPK inhibitor (EMD Millipore, 506148) in 4% DMSO was added to achieve designated concentrations or 2.5 μL of DMSO was added as control. After 1 h incubation at 37 °C, 2.5 μL of inducers including thapsigargin, 2-cyano-3,12-dioxooleana-1,9-dien-28-imidazolide (CDDO-IM, Toronto Research Chemicals Inc., C228090), ionomycin (Life Technologies, I-24222), or MG132 (Sigma-Aldrich, C2211) in 2% DMSO was added to reach a corresponding concentration and 2.5 μL of 2% DMSO was used as control. The plates were incubated for 18 h, and the reporter signal was recorded with a BMG POLARstar Omega plate reader in luminescence mode after adding 25 μL of Steady-Glo luciferase assay reagent (Promega, E2510). Wells treated with compounds only but no inducers were used as background controls correspondingly, and wells treated with inducers but no compounds were used as 100% controls. The RLU (% of control) = 100 × (well value − average of background)/(average of 100% control − average of background). These data were analyzed by using EXCEL software. The experiments were replicated at least three times, and are presented as the average ± SEM.

Statistical Analysis. Statistical comparisons of mean values were performed using one-way analysis of variance (ANOVA). $P < 0.05$ was considered to be statistically significant.

ADME Assays. *Plasma Stability Assay.* Plasma from male C57BL/6 mice was obtained from BioReclamation (cat # MSEPLNAHP-C57-M), diluted 1:1 with PBS, and warmed to 37 °C. Compounds (10 mM in DMSO) were added to a final concentration of 1 μM. Zero time point samples were immediately removed and quenched with a solution of 5 parts acetonitrile to 1 part water. The remaining compound/serum mixture was incubated for 3 h at 37 °C with shaking. End point samples were taken and mixed with 5 parts acetonitrile to 1 part water. Following quenching, all samples were centrifuged at 1000*g* for 10 min. Supernatants were further mixed with ACN containing 1.25 μM indomethacin, which was used as an internal standard, and centrifuged again at 1000*g* for 10 min. Samples were transferred to autosampler vials (Shimadzu Prominence HPLC) and quantified on an Applied Biosystems Sciex API 3000 triple quadrupole mass spectrometer in MRM mode.

Microsomal Stability Assay. Pooled mouse liver microsomes from Xenotech (cat # M1000) were briefly warmed to 37 °C and incubated with test compounds for 10 min. NADPH was added to a final concentration of 2 mM. Final concentrations of compounds and microsomal protein were 4 μM and 1 μg/μL, respectively. Zero time point samples were taken immediately following addition of NADPH and quenched with 5 parts acetonitrile to 1 part water. Compounds were incubated with microsomes and NADPH for 1 h at 37 °C with shaking. End point samples were mixed with 5 parts acetonitrile to 1 part water. All samples were centrifuged at 1000*g* for 10 min following quenching. Supernatants were mixed with ACN containing 1.25 μM indomethacin (used as an internal standard) and subsequently centrifuged at 1000*g* for 10 min. Samples were pipetted into autosampler tubes (Shimadzu Prominence HPLC) and analyzed using an Applied Biosystems Sciex API 3000 triple quadrupole mass spectrometer in MRM mode.

Parallel Artificial Membrane Permeability Assay (PAMPA). For PAMPA experiments, 96-well multiscreen acceptor filter plates with 0.45 μM Immobilon-P membranes (Millipore # MAIPNTR10) were coated with the polar lipid 1,2-dioleoyl-*sn*-glycero-3-phosphocholine (Avanti # 145414) and incubated for 10 min. Test compounds were diluted to 100 μM in aqueous pH 7.4 buffer (Fisher # SB110-1), and 150 μL of diluted compound was added to each well. Multiscreen transport receiver plates (Millipore # MAIRNPS50) were filled with 300 μL of aqueous pH 7.4 buffer (Fisher # SB110-1). Multiscreen acceptor filter plates containing compound were then coupled to the receiver plates and incubated at room temperature for 20 h. Equilibrium controls were obtained by combining the same compound and buffer solutions without the presence of a membrane. The amount of compound in the acceptor plate and equilibrium solutions was determined using an Applied Biosystems Sciex API 3000 triple quadrupole mass spectrometer. These concentrations were used to calculate the permeability (log P_e) of the compounds using the following equation: $\log P_e = \log\{C - \ln(1 - [\text{drug}]_{\text{acceptor}}/[\text{drug}]_{\text{equilibrium}})\}$, where $C = (V_D V_A)/((V_D + V_A)\text{area} \times \text{time})$.

■ ASSOCIATED CONTENT

Ⓢ Supporting Information

Additional table showing PDSP off-target binding data for **4hh**. This material is available free of charge via the Internet at http://pubs.acs.org.

■ AUTHOR INFORMATION

Corresponding Author

*E-mail: ncosford@sanfordburnham.org.

DOI: 10.1021/cn500297v
ACS Chem. Neurosci. 2015, 6, 464−475

Funding

This work was supported by NIH Grant HG005033 (NIGMS/NIMH), the Department of Defense Amyotrophic Lateral Sclerosis Research Program under Award Number W81XWH-12-1-0373 (to N.D.P.C.), and Janssen Research and Development LLC.

Notes

The authors declare no competing financial interest.

■ ACKNOWLEDGMENTS

We would like to thank Dr. Nicholas Carruthers (Janssen Research and Development LLC) for helpful comments. The binding profile for compound **4hh** was generously provided by the National Institute of Mental Health's Psychoactive Drug Screening Program, Contract HHSN-271-2008-00025-C (NIMH PDSP).

■ DEDICATION

This paper is dedicated to our departed colleague Professor Gregory P. Roth.

■ ABBREVIATIONS

6-OHDA, 6-hydroxydopamine; ADME, absorption, distribution, metabolism and excretion; ALS, amyotrophic lateral sclerosis; AP1, transcription activator protein 1; ASK1, apoptosis signal regulating kinase 1; ATF6, activating transcription factor 6; BBB, blood-brain barrier; CDDO, 2-cyano-3,12-dioxooleana-1,9-dien-28-oic acid; CHOP, C/EBP homologous protein; DDTD, 3′,4′-dichloro-3-(3,4-dichlorophenylacetyl)-2,4,6-trihydroxydeoxybenzoin; DTT, dithiothreitol; ER, endoplasmic reticulum; IRE1, inositol-requiring enzyme 1; JNK, c-Jun N-terminal kinase; MAP, mitogen-activated protein; MG132, carbobenzoxy-Leu-Leu-leucinal; MOA, mode of action; p38, p38 MAP kinase; PAMPA, parallel artificial membrane permeability assay; PERK, protein kinase (PKR)-like ER kinase; POC, proof-of-concept; SAR, structure−activity relationship; SERCA, sarco/endoplasmic reticulum Ca^{2+} ATPase; SOD1, superoxide dismutase 1; TRAF2, tumor necrosis factor receptor-associated factor 2; UPR, unfolded protein response

■ REFERENCES

(1) Doyle, K. M., Kennedy, D., Gorman, A. M., Gupta, S., Healy, S. J., and Samali, A. (2011) Unfolded proteins and endoplasmic reticulum stress in neurodegenerative disorders. *J. Cell. Mol. Med. 15*, 2025−2039.

(2) Minamino, T., Komuro, I., and Kitakaze, M. (2010) Endoplasmic reticulum stress as a therapeutic target in cardiovascular disease. *Circ. Res. 107*, 1071−1082.

(3) Oyadomari, S., and Mori, M. (2004) Roles of CHOP/GADD153 in endoplasmic reticulum stress. *Cell Death Differ. 11*, 381−389.

(4) Nishitoh, H., Kadowaki, H., Nagai, A., Maruyama, T., Yokota, T., Fukutomi, H., Noguchi, T., Matsuzawa, A., Takeda, K., and Ichijo, H. (2008) ALS-linked mutant SOD1 induces ER stress- and ASK1-dependent motor neuron death by targeting Derlin-1. *Genes Dev. 22*, 1451−1464.

(5) Kim, I., Xu, W., and Reed, J. C. (2008) Cell death and endoplasmic reticulum stress: disease relevance and therapeutic opportunities. *Nat. Rev. Drug Discovery 7*, 1013−1030.

(6) Bravo, R., Parra, V., Gatica, D., Rodriguez, A. E., Torrealba, N., Paredes, F., Wang, Z. V., Zorzano, A., Hill, J. A., Jaimovich, E., Quest, A. F., and Lavandero, S. (2013) Endoplasmic reticulum and the unfolded protein response: dynamics and metabolic integration. *Int. Rev. Cell Mol. Biol. 301*, 215−290.

(7) Nishitoh, H., Matsuzawa, A., Tobiume, K., Saegusa, K., Takeda, K., Inoue, K., Hori, S., Kakizuka, A., and Ichijo, H. (2002) ASK1 is essential for endoplasmic reticulum stress-induced neuronal cell death triggered by expanded polyglutamine repeats. *Genes Dev. 16*, 1345−1355.

(8) Urano, F., Wang, X., Bertolotti, A., Zhang, Y., Chung, P., Harding, H. P., and Ron, D. (2000) Coupling of stress in the ER to activation of JNK protein kinases by transmembrane protein kinase IRE1. *Science 287*, 664−666.

(9) Wang, X. Z., and Ron, D. (1996) Stress-induced phosphorylation and activation of the transcription factor CHOP (GADD153) by p38 MAP Kinase. *Science 272*, 1347−1349.

(10) Davis, R. J. (2000) Signal transduction by the JNK group of MAP kinases. *Cell 103*, 239−252.

(11) DuRose, J. B., Tam, A. B., and Niwa, M. (2006) Intrinsic capacities of molecular sensors of the unfolded protein response to sense alternate forms of endoplasmic reticulum stress. *Mol. Biol. Cell 17*, 3095−3107.

(12) Yoshida, H. (2007) ER stress and diseases. *FEBS J. 274*, 630−658.

(13) Supnet, C., and Bezprozvanny, I. (2010) The dysregulation of intracellular calcium in Alzheimer disease. *Cell Calcium 47*, 183−189.

(14) Yu, J. T., Chang, R. C., and Tan, L. (2009) Calcium dysregulation in Alzheimer's disease: from mechanisms to therapeutic opportunities. *Prog. Neurobiol. 89*, 240−255.

(15) Zundorf, G., and Reiser, G. (2011) Calcium dysregulation and homeostasis of neural calcium in the molecular mechanisms of neurodegenerative diseases provide multiple targets for neuroprotection. *Antioxid. Redox Signal. 14*, 1275−1288.

(16) Hoozemans, J. J., Veerhuis, R., Van Haastert, E. S., Rozemuller, J. M., Baas, F., Eikelenboom, P., and Scheper, W. (2005) The unfolded protein response is activated in Alzheimer's disease. *Acta Neuropathol. 110*, 165−172.

(17) Imai, Y., Soda, M., and Takahashi, R. (2000) Parkin suppresses unfolded protein stress-induced cell death through its E3 ubiquitin-protein ligase activity. *J. Biol. Chem. 275*, 35661−35664.

(18) Kikuchi, H., Almer, G., Yamashita, S., Guegan, C., Nagai, M., Xu, Z., Sosunov, A. A., McKhann, G. M., 2nd, and Przedborski, S. (2006) Spinal cord endoplasmic reticulum stress associated with a microsomal accumulation of mutant superoxide dismutase-1 in an ALS model. *Proc. Natl. Acad. Sci. U. S. A. 103*, 6025−6030.

(19) Limpert, A. S., Mattmann, M. E., and Cosford, N. D. (2013) Recent progress in the discovery of small molecules for the treatment of amyotrophic lateral sclerosis (ALS). *Beilstein J. Org. Chem. 9*, 717−732.

(20) Kim, I., Shu, C. W., Xu, W., Shiau, C. W., Grant, D., Vasile, S., Cosford, N. D., and Reed, J. C. (2009) Chemical biology investigation of cell death pathways activated by endoplasmic reticulum stress reveals cytoprotective modulators of ASK1. *J. Biol. Chem. 284*, 1593−1603.

(21) Chen, J. T., Fong, Y. C., Li, T. M., Liu, J. F., Hsu, C. W., Chang, C. S., and Tang, C. H. (2008) DDTD, an isoflavone derivative, induces cell apoptosis through the reactive oxygen species/apoptosis signal-regulating kinase 1 pathway in human osteosarcoma cells. *Eur. J. Pharmacol. 597*, 19−26.

(22) Lytton, J., Westlin, M., and Hanley, M. R. (1991) Thapsigargin inhibits the sarcoplasmic or endoplasmic reticulum Ca-ATPase family of calcium pumps. *J. Biol. Chem. 266*, 17067−17071.

(23) Hail, N., Jr., Konopleva, M., Sporn, M., Lotan, R., and Andreeff, M. (2004) Evidence supporting a role for calcium in apoptosis induction by the synthetic triterpenoid 2-cyano-3,12-dioxooleana-1,9-dien-28-oic acid (CDDO). *J. Biol. Chem. 279*, 11179−11187.

(24) Liu, C., and Hermann, T. E. (1978) Characterization of ionomycin as a calcium ionophore. *J. Biol. Chem. 253*, 5892−5894.

(25) Shimizu, S., Kadowaki, M., Yoshioka, H., Kambe, A., Watanabe, T., Kinyamu, H. K., and Eling, T. E. (2013) Proteasome inhibitor MG132 induces NAG-1/GDF15 expression through the p38 MAPK pathway in glioblastoma cells. *Biochem. Biophys. Res. Commun. 430*, 1277−1282.

DOI: 10.1021/cn500297v
ACS Chem. Neurosci. 2015, 6, 464−475

(26) Grosskreutz, J., Van Den Bosch, L., and Keller, B. U. (2010) Calcium dysregulation in amyotrophic lateral sclerosis. *Cell Calcium 47*, 165−174.
(27) Lautenschlager, J., Prell, T., Ruhmer, J., Weidemann, L., Witte, O. W., and Grosskreutz, J. (2013) Overexpression of human mutated G93A SOD1 changes dynamics of the ER mitochondria calcium cycle specifically in mouse embryonic motor neurons. *Exp. Neurol. 247*, 91−100.
(28) Tadic, V., Prell, T., Lautenschlaeger, J., and Grosskreutz, J. (2014) The ER mitochondria calcium cycle and ER stress response as therapeutic targets in amyotrophic lateral sclerosis. *Front. Cell. Neurosci. 8*, 147.
(29) Van Den Bosch, L., Vandenberghe, W., Klaassen, H., Van Houtte, E., and Robberecht, W. (2000) Ca^{2+}-permeable AMPA receptors and selective vulnerability of motor neurons. *J. Neurol. Sci. 180*, 29−34.
(30) Palecek, J., Lips, M. B., and Keller, B. U. (1999) Calcium dynamics and buffering in motoneurones of the mouse spinal cord. *J. Physiol. 520* (Pt 2), 485−502.

DOI: 10.1021/cn500297v
ACS Chem. Neurosci. 2015, 6, 464−475